PAIRED ACCELERATED FRAMES: THE PERFECT INTERFEROMETER WITH EVERYWHERE SMOOTH WAVE AMPLITUDES*

ULRICH H. GERLACH
Department of Mathematics, Ohio State University, Columbus, OH 43210, USA

In the absence of gravitation the distinguishing feature of any linearly and uniformly accelerated frame is that it is one member of a pair moving into opposite directions. This pairing partitions Minkowski spacetime into four mutually exclusive and jointly exhaustive domains whose boundary consists of the future and past event horizons relative to each of the two frames. This acceleration-induced partitioning of spacetime leads to a nature-given interferometer. It accommodates quantum mechanical and wave mechanical processes in spacetime which in (Euclidean) optics correspond to wave processes in a "Mach-Zehnder" interferometer: amplitude splitting, reflection, and interference. The spacetime description of these processes is given in terms of amplitudes which are defined globally as well as locally in each of the four Rindler spacetime domains. It is found that these amplitudes behave smoothly across the event horizons. In this context there arises quite naturally a complete set of orthonormal wave packet histories, one of whose key properties is their *explosivity index*. It measures the rate at which the wave packets collapse and re-explode. In the limit of low index values the wave packets trace out fuzzy world lines. For large mass this fuzziness turns into the razor-sharpness of classically determinate world lines of the familiar Klein-Gordon scalar particles. By contrast, in the asymptotic limit of high index values, there are no world lines, not even fuzzy ones. Instead, the wave packet histories are those of entities with non-trivial internal collapse and explosion dynamics. Their details are described by the wave processes in the above-mentioned Mach-Zehnder interferometer. Each one of them is a double slit interference process. These wave processes are applied to elucidate the amplification of waves in an accelerated inhomogeneous dielectric. Also discussed are the properties and relationships among the transition amplitudes of an accelerated finite-time detector.
PACS numbers: 04.62.+v, 03.65.Pm, 42.25.Hz, 42.25.Fx

I. INTRODUCTION

The fundamental feature of uniformly and linearly accelerated observers is that they come in pairs. If the spacetime of one accelerated frame is

$$\left.\begin{array}{l} t-t_0=\xi\sinh\tau \\ z-z_0=\xi\cosh\tau \end{array}\right\} \quad \text{"Rindler Sector I"} \quad , \tag{1}$$

then the spacetime of its twin is

$$\left.\begin{array}{l} t-t_0=-\xi\sinh\tau \\ z-z_0=-\xi\cosh\tau \end{array}\right\} \quad \text{"Rindler Sector II"} \quad . \tag{2}$$

These two regions of spacetime are causally disjoint. Their event horizons $t-t_0=\pm|z-z_0|$ separate these regions from their chronological future F,

$$\left.\begin{array}{l} t-t_0=\xi\cosh\tau \\ z-z_0=\xi\sinh\tau \end{array}\right\} \quad \text{"Rindler Sector F"} \quad , \tag{3}$$

and their chronological past P,

$$\left.\begin{array}{l} t-t_0=-\xi\cosh\tau \\ z-z_0=-\xi\sinh\tau \end{array}\right\} \quad \text{"Rindler Sector P"} \quad . \tag{4}$$

*Published in Phys. Rev. D **59**, 104009 (1999) and based in part on a talk given at the Sixth Midwestern Relativity Conference, St. Louis, November 13-14,1997, and on part of a report given in the session "Casimir Effect" originally published in the Proc. of the Eighth Marcel Grossmann Meeting on General Relativity, Jerusalem, June 23-27, 1997, edited by Tsvi Piran (World Scientific, Singapore, 1999)

We always assume that $\xi > 0$. Thus, as shown in Figure 1, an accelerated observer induces a partitioning of Minkowski spacetime into the four Rindler sectors I, II, F and P.

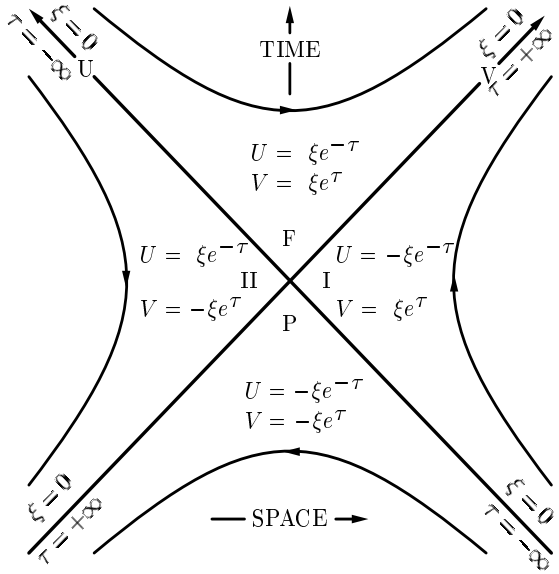

FIG. 1. Acceleration-induced partitioning of spacetime into the four Rindler sectors.

This partitioning opens a new perspective for relativistic processes governed by the Klein-Gordon wave equation: *The four Rindler sectors form a perfect interferometer.*

A. Lorentzian Mach-Zehnder Interferometer

More precisely, the two accelerating frames ($I\&II$) serve as the two coherent legs of a Lorentzian version of the Mach-Zehnder interferometer [1]. As indicated in Figure 2, the two well-known pseudo-gravitational potentials in these frames serve as the two mirrors with 100% reflectivity. The two spacetime regions in the future F and the past P *near* the intersection ("bifurcation event") of the event horizons serve as "half-silvered" mirrors. A wave in P *far* from the bifurcation event enters the "interferometer" from P. One can show mathematically, and this is done in Figures 5 and 7, that near the two event horizons $t - t_0 = -|x - x_0|$ the wave splits into two partial waves: one propagates across

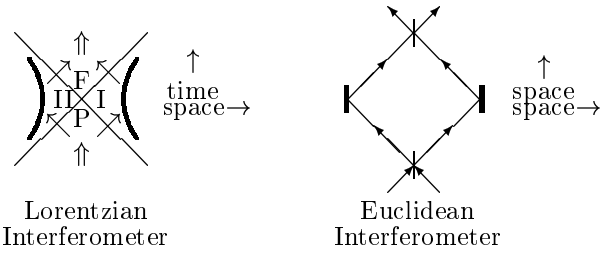

FIG. 2. Two interferometers. The Euclidean interferometer, which in optics is known as a Mach-Zehnder interferometer, consists of a half-silvered entrance mirror (thin line at the bottom), a half-silvered exit mirror (thin line at the top), and two fully reflecting mirrors (thick lines on the right and the left). The Lorentzian interferometer consists of the entrance region, Rindler Sector P, the exit region, Rindler Sector F, and the two reflective regions, Rindler Sectors I and II. The reflection is brought about by by the pseudo-gravitational potential (see Eq. (14)) in each sector. The thick hyperbolas separate the region of this potential where the mode is oscillatory from that region where it is evanescent. This reflection process is detailed in Figure 6.

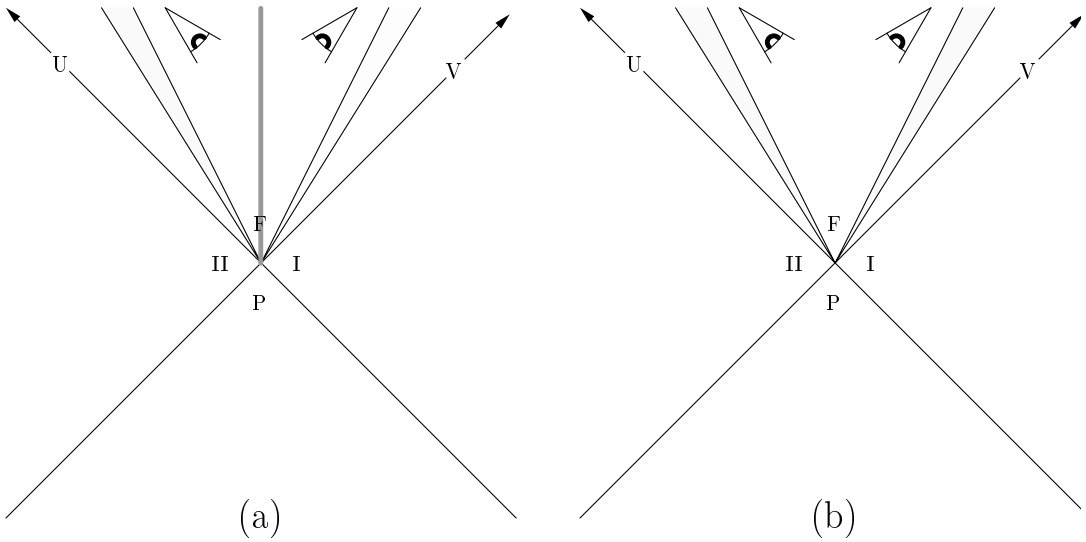

FIG. 3. Pair of monochromatic detectors (located at $\tau = c_1$ and $\tau = c_2$) configured to measure interference between waves from I and II, Figure (a), or to measure the amplitude of each waves from I and II separately, Figure (b) ("delayed choice experiment"). The detectors are monochromatic because they are surrounded by interference filters. Each such filter consists of a Fabry-Perot cavity with uniformly moving walls. Such a cavity has discrete transmission resonances at Rindler frequencies given by $\omega = n\pi/\tanh^{-1}\beta, \quad n = 1, 2, \cdots$, where β is the relative velocity of the cavity walls. Their histories delineate the evolution of a cavity's interior (lightly shaded wedge in the figure).

the past event horizon, enters Rindler Sector I. There it gets reflected by the Lorentz invariant pseudo-gravitational potential. This reflection is demonstrated mathematically in Figures 6 and 7. The other partial wave suffers the analogous reflection in Rindler Sector II. The two partial waves cross the event horizons $t - t_0 = |x - x_0|$ and, as shown in Figure 5, recombine in Rindler Sector F. There these waves are intercepted by two freely floating detectors configured to perform a time-plus-space version of Wheeler's "delayed choice" experiment [2]. This means that an (inertial) physicist who spends his life in Rindler Sector F

(a) releases two free-float particle detectors whose apertures point into opposite directions.

(b) places between them a free-float mirror with freely chosen reflective properties. See Figure 3.

A brief parenthetical remark is in order: When we say "inertial physicist in F", "free-float particle detector in F", and so on, what we mean is that the separation between their straight world lines increases at a constant rate. Moreover, at each instant of their common proper elapsed time ($0 < \xi$) these entities are situated on a spacelike hypersurface whose points are (τ, y, x) $(-\infty < \tau, y, x < \infty)$, and whose neighborhoods are metrically equivalent ("isometric") to one another.

The chosen reflectivity of the mirror determines what the detectors will measure. If the reflectivity is between zero and one (Figure 3a), then the detectors respond to the interfering amplitudes of the waves coming from I and II. If the reflectivity is zero (mirror is perfectly transparent, Figure 3b), then the detectors respond to the respective amplitudes of the waves coming separately from I and II.

The "delayed choice" feature enters when the wave intensity is so low that the individuality of the quanta occupying the wave starts to manifest itself. Under this circumstance a quantum could be found still propagating in I and/or II, while the physicist is making up his/her mind whether or not to place a mirror between the two particle detectors in Figure 3.

Like its Euclidean relative, the Lorentzian Mach-Zehnder interferometer (I, II, P, F) is an amplitude splitting device. It also has the advantage that the two paths for the two amplitudes traverse regions which are spacious and far apart. This is why it is of interest to the physicists. These regions, Rindler I and Rindler II, can, for example, accommodate a pair of accelerated dielectrics or a gravitational disturbance. Either one would alter the interference between the amplitudes when they recombine in Rindler sector F. As a result antiparticles are produced. This is demonstrated in Section X.

The mathematicians find this Lorentzian interferometer appealing for its mathematical simplicity. They notice that it is a device which is Lorentz boost-invariant in the absence of gravitational disturbances. As a consequence, the evolution process of an arbitrary wave function, making its way from P to F via I and II, is by necessity simply a superposition of elementary processes. Each one of them is easy to follow because each one is a boost-invariant Cauchy evolution of the Klein-Gordon equation

$$\frac{\partial^2\psi}{\partial t^2} - \frac{\partial^2\psi}{\partial z^2} + k^2\psi = 0, \tag{5}$$

where $k^2 = k_x^2 + k_y^2 + m^2c^2/\hbar^2$. Physically speaking, ψ is the electric (resp. magnetic) field perpendicular to the x and y directions of the T.M. (resp. T.E.) modes [3–5] whenever $m = 0$.

B. Two Fundamental Sets of Boost-Invariant Modes

These elementary Cauchy evolutions are fundamental. Each one describes an independent Mach-Zehnder beam-splitting and (subsequent) interference process. Furthermore, they serve as a foundation for carrying the imprints of gravitational disturbances that might be present in I and/or II [6].

These Cauchy evolutions are Fourier transforms of the planewave states

$$e^{\mp i[(t-t_0)k\cosh\theta + (z-z_0)k\sinh\theta]} \equiv e^{\mp ik(Ve^{\theta} + Ue^{-\theta})/2} \tag{6}$$

of either positive (upper sign) or negative (lower sign) Minkowski frequency. These states, we recall, are parametrized by the "pseudo" angular parameter θ ("Minkowski frequency parameter") on the mass hyperboloid $\omega_k^2 - k_z^2 = k_x^2 + k_y^2 + m^2c^2/\hbar^2 \equiv k^2$,

$$\omega_k = k\cosh\theta > 0 \tag{7}$$
$$k_z \ = k\sinh\theta \quad , \tag{8}$$

and we are introducing for the sake of mathematical efficiency

$$U = \quad (t-t_0) - (z-z_0) \tag{9}$$
$$V = (t-t_0) + (z-z_0) \quad , \tag{10}$$

the familiar null coordinates.

These elementary Cauchy evolutions, call them $B_\omega^\pm$, are partial waves. They are defined so that their superposition

$$\int_{-\infty}^{\infty} B_\omega^\pm(kU, kV)e^{-i\omega\theta}\ d\omega \equiv e^{\mp i[(t-t_0)k\cosh\theta + (z-z_0)k\sinh\theta]} \tag{11}$$

constitutes a partial wave representation of each planewave mode, Eq.(6). Consequently, these partial wave modes are Fourier transforms on the mass hyperboloid and they come in pairs,

$$B_\omega^\pm(kU, kV) = \frac{1}{2\pi}\int_{-\infty}^{\infty} e^{\mp ik(Ve^{\theta} + Ue^{-\theta})/2}e^{i\omega\theta}d\theta \quad , \tag{12}$$

one of purely positive (upper sign), the other of purely negative (lower sign) Minkowski frequency. Both are boost invariant, that is to say, they are eigenfunctions of the "boost energy" operator

$$i\frac{\partial}{\partial\tau} \equiv i\left[(z-z_0)\frac{\partial}{\partial t} + (t-t_0)\frac{\partial}{\partial z}\right] = i\left[V\frac{\partial}{\partial V} - U\frac{\partial}{\partial U}\right] \tag{13}$$

with eigenvalue ω. Furthermore, as one sees from Figures 4a and 4b, in each of the Rindler sectors they are represented by the various kinds of Bessel functions. For this reason we shall refer to them as "Minkowski-Bessel" states or modes or distributions, depending on the context.

Given their fundamental role, we must make sure that the two kinds of Minkowski-Bessel states are well-defined physically *and* mathematically.

Note that the modes $B_\omega^\pm$ are defined globally on Minkowski spacetime, but as shown in Figures 4a and 4b they have Rindler coordinate representatives which are only defined in the interior of each Rindler sector, where they satisfy

$$\left(\xi\frac{\partial}{\partial\xi}\xi\frac{\partial}{\partial\xi} - \frac{\partial^2}{\partial\tau^2} \mp k^2\xi^2\right)\psi = 0 \quad \begin{cases} - : & \text{"Rindler Sector I or II"} \\ + : & \text{"Rindler Sector F or P"} \end{cases} , \tag{14}$$

where, as a consequence, one finds in Rindler I and II the "pseuso-gravitational potential" ($\propto k\xi$) already mentioned several times, and where these coordinate representatives are proportional to one or the other of the two kinds of

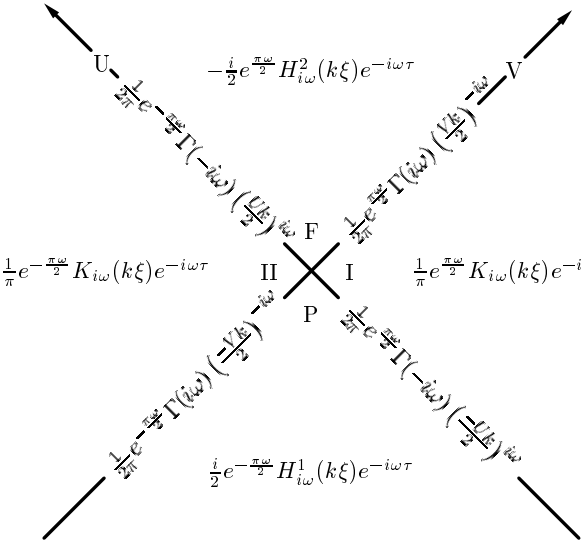

FIGURE (a)

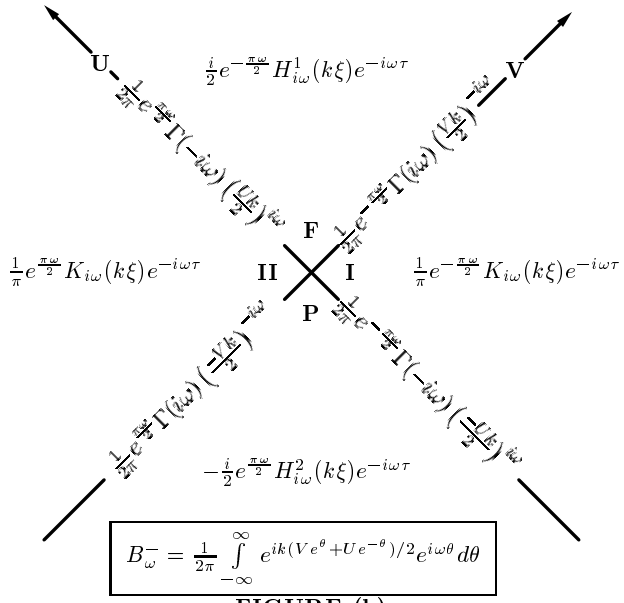

FIGURE (b)

FIG. 4. Minkowski-Bessel modes of positive and negative Minkowski frequency, and the four Rindler coordinate representatives for each. Note that the ensuing Figures 5, 6, and 7 are mathematically equivalent to the above figures (Figs. 4a and b). All of them depict the Minkowski-Bessel modes $B^{\pm}_{\omega}$. Figure 6 is obtained by applying to Figure 4 some well-known identities between Hankel and Bessel functions and between McDonald and modified Bessel functions. Figures 5 and 6 are equivalent by virtue of the coordinate transformations in Figure 1. Figure 7 is the WKB-approximate form of Figure 5.

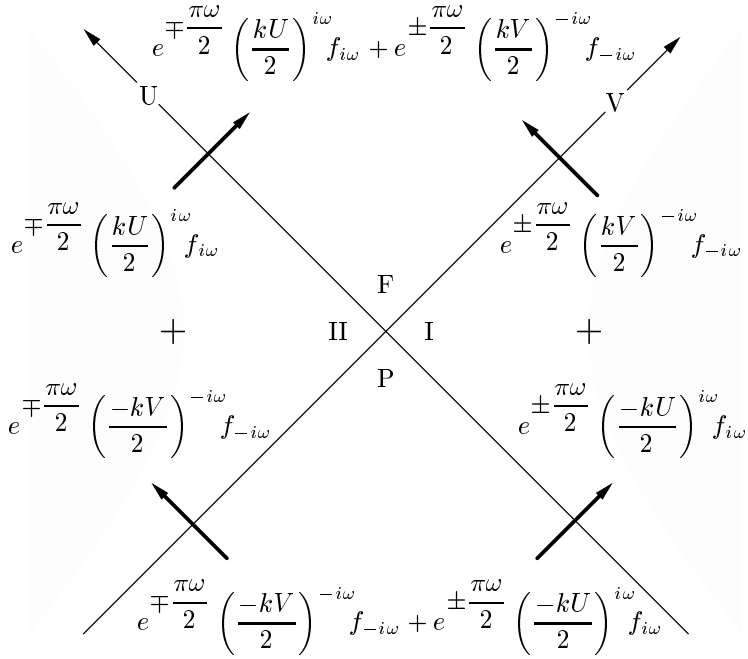

FIG. 5. Amplitude splitting of the Minkowski-Bessel modes of positive and negative Minkowski frequency. Each mode expresses an interference process as found in the Mach-Zehnder interferometer familiar from optics. A wave in P *far* from the bifurcation event enters the "interferometer" from P. As indicated by the two heavy arrows, the wave splits into two partial waves: one propagates from P (tail of the arrow) across the past event horizon, and enters Rindler Sector I (tip of the same arrow). There it propagates to the right under the influence of the familiar boost-invariant pseudo-gravitational potential. This is shown explicitly in Figure 6. The wave becomes evanescent (exponentially decaying) in the shaded hyperbolic region and hence gets reflected by this potential. Upon propagating to the left the wave escapes from Rindler Sector I (tail of the next arrow) through its future event horizon into the future sector F (tip of that arrow). There it recombines with the other partial wave which got reflected in Rindler Sector II.

Hankel functions ($H^{(1)}_{i\omega}$ or $H^{(2)}_{i\omega}$ in P and F) or the MacDonald function ($K_{i\omega}$ in I and II). On the acceleration induced event horizons, the boundary ($UV = 0$) of these sectors, the Rindler time coordinate τ becomes pathological and so do these functions: they oscillate so rapidly that they have no definite value on the event horizons $\xi = 0$. This is true even when one uses the well behaved null coordinates U and V. See Figure 5.

For obvious reasons such a "pathological" behavior seems to be troubling, both physically and mathematically. In fact, the literature, as well as discussions with workers in the field, have emphasized this pejorative assessment by implicitly and explicitly describing the behaviour of the these Minkowski-Bessel modes across the event horizon as being "singular" or "highly singular". All this has lent credence to the misconception that these modes are physically unrealistic and mathematically unjustified ways of coming to grips with natural phenomena associated with pairs of accelerated frames.

Furthermore, the highly oscillatory (non-analytic) behaviour of $B^{\pm}_{\omega}(kU, kV)$ at $U = V = 0$ has been used, erroneously, as an indicator to signal the mixing of positive and negative Minkowski frequencies [7].

The purpose of this article is to dispel these mathematical and physical misconceptions. This turns out to be a fruitful endeavor for additional reasons, which are theoretical and (hence also) practical: By placing the Minkowski-Bessel modes into their wider mathematical framework one can assess their status in our hierarchy of knowledge. Furthermore, this wider framework also leads to a complete set of globally well-behaved orthonormal wavepackets, which (i) serve as the connecting link between quantum mechanical wave functions and the razor-sharp world lines of classical mechanics and (ii) open the door to probing the structure of spacetime with probes (exploding wave packets, Section VII.C.2) which are as yet unexplored.

II. TWO COMPLEMENTARY POINTS OF VIEW

The Minkowski-Bessel modes oscillate very rapidly near the event horizon. The erroneous assessment of this behavior as "pathological" is tied up in their very description as "modes" and is a direct consequence of the concomitant and frequently asked question: "What is the behavior of one of these modes at the origin $U = V = 0$ where the two event horizons intersect?" or "What is its behavior as one passes across one of the event horizons $|t - t_0| = |z - z_0|$?" These are questions that pertain to the continuity or smoothness of the normal mode amplitudes.

Questions like these are a consequence of the *conventional viewpoint*. It regards $B^{\pm}_{\omega}(kU, kV)$ given by Eqs.(12) and depicted in Figures 4a and 4b (or in Figures 5, 6, and 7) as "normal modes", and thereby asks for their amplitudes as one varies (U, V) while keeping the parameter ω fixed.

This viewpoint will suffice if one's attention is limited to the interior of anyone of the four Rindler sectors I, II, F, or P. In that case one has four ordinary functions, the coordinate representatives of $B^{+}_{\omega}(kU, kV)$, and another four for $B^{-}_{\omega}(kU, kV)$, as depicted in Figures 4a and 4b.

However, we also need to know the amplitude on the boundary (event horizons) between the Rindler sectors. For that, the conventional viewpoint is deficient in that it forces us not only into asking mathematically meaningless questions, but also into referring to "properties" of the field which are physically immeasurable.

By contrast, the *complementary viewpoint* regards $B^{\pm}_{\omega}(kU, kV)$ as functions of ω and views U and V as parameters. The superiority of this viewpoint lies in that it allows us to extend our familiar notion of ordinary functions to *generalized* functions, which are well-defined even when (U, V) lies on the boundary.

These generalized functions ("distributions") (i) subsume ordinary functions (of ω) as a special case, and (ii) are continuous and smoothly parametrized not only when (U, V) lies on the boundary between any pair of Rindler sectors, but also when $U = V = 0$, the intersection of the two event horizons. Furthermore, unlike a (monochromatic) normal mode, a generalized function expresses mathematically what is measured physically.

III. ARE GENERALIZED FUNCTIONS PHYSICALLY NECESSARY?

Before identifying the two families of generalized functions we must ask: What fact(s) of reality give rise to these generalized functions? i.e., Do they have a natural origin, and if so, what is it? A brief answer lies in the following two observation:

First of all, in nature one does not find translation and boost eigenfunctions (of infinite extent and infinitely sharp momentum) as such. Instead, one only observes wave packets of finite (although possibly quite large) extent and of fuzzy (although possibly quite sharp) momentum. See Section VII. Nevertheless, translation and boost invariance *are* physical properties found in nature, and for good reasons it is necessary to express them in terms of translation and boost eigenfunctions. In order to harmonize the conflict between this necessity and what is observed, physicists and mathematicians have enlarged the concept of an eigenfunction into the more sophisticated concept of a *generalized*

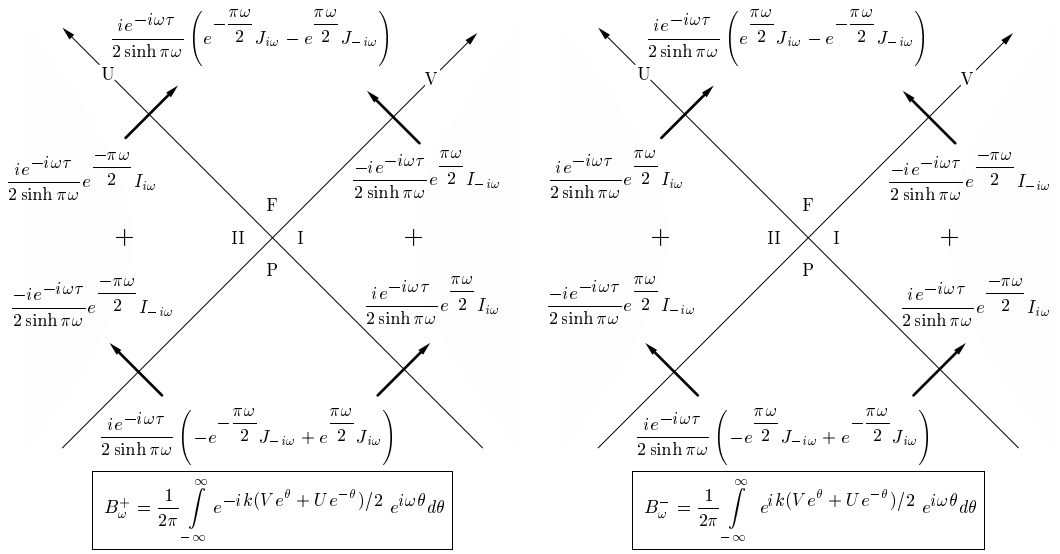

FIG. 6. Reflection of partial waves from their potential barriers (shaded hyperbolas) in Rindler Sectors I and II. As in Figure 5, the four arrows connect partial waves propagating from one Rindler sector to another. In Rindler Sectors P and F the partial waves are proportional to the Bessel functions $J_{\pm i\omega}(k\xi)$ of order $\pm i\omega$, while in I and II they are proportional to the modified Bessel functions $I_{\pm i\omega}(k\xi)$. The latter oscillate for finite $k\xi$, but blow up exponentially as $k\xi \to \infty$ in each hyperbolically shaded region. The reflection process is brought about by the boundary condition that the incident wave in I ($\propto I_{i\omega}(k\xi)$) must combine with the reflected wave ($\propto I_{-i\omega}(k\xi)$) so as to form a total wave whose amplitude approaches zero as $k\xi \to \infty$. This wave is a standing wave ($\propto (I_{i\omega}(k\xi) - I_{-i\omega}(k\xi))$ in I and thus expresses a process of reflection from the boost-invariant pseudo-gravitational potential. An analogous reflection process takes place in Rindler Sector II.

eigenfunction, i.e. an *eigendistribution*. Thus for physical and mathematical reasons the translation and boost invariance in nature must actually be formulated in terms of generalized functions. Ordinary functions won't do. Without generalized functions there would not exist, for example, a globally defined solution to the Klein-Gordon equation which is Lorentz invariant.

Secondly, there is an equally, if not more, urgent reason for introducing them: The general solution to the Klein-Gordon equation is a linear combination of the two sets of Minkowski-Bessel modes, Eq.(12)

$$\psi = \int_{-\infty}^{\infty} [\phi^+(\omega)\ B_\omega^+(kU, kV) + \phi^-(\omega)\ B_\omega^-(kU, kV)]\ d\omega \quad . \tag{15}$$

The two functions $\phi^{\pm}(\omega)$ comprise an $SU(1,1)$ two-spinor field [6] over the Rindler frequency domain $-\infty < \omega < \infty$. It is difficult to overstate the importance of this spinor field. Its Stokes parameters (= expectation values of the Pauli matrices) form a vector field which (a) carries the imprints of gravitation, and (b) has the Eotvos property of being independent of the mass of the Klein-Gordon particle [6]. This fundamental role of the spinor field demands that the solution represented by Eq.(15) be globally well-defined, including at events on the event horizon $UV = 0$.

Thus the motivation for considering the two Minkowski-Bessel distributions and their test function spaces comes not only from mathematical analysis but also from physics and geometry.

IV. MATHEMATICAL TUTORIAL: TWO FAMILIES OF GENERALIZED FUNCTIONS

Generalized functions are a familiar part of the mathematical landscape [8]. Nevertheless, there seems to be lacking a readily accessible mathematical framework which accommodates the boost-invariant and globally defined eigenmodes of the Klein-Gordon equation. The purpose of this section is to remedy this lack.

$$\text{PHASES:} \left\{ \begin{array}{l} \mathcal{S}^U = \omega \ln(\omega + \sqrt{\omega^2 + k^2 UV}) - \sqrt{\omega^2 + k^2 UV} - \omega \ln k|U| - \frac{\pi}{4} \\ \mathcal{S}^V = \omega \ln(\omega + \sqrt{\omega^2 + k^2 UV}) - \sqrt{\omega^2 + k^2 UV} - \omega \ln k|V| - \frac{\pi}{4} \end{array} \right.$$

$$\text{AMPLITUDE} = \left[\frac{1}{2\pi\sqrt{\omega^2 + k^2 UV}} \frac{e^{\pi\omega}}{2\sinh \pi\omega} \right]^{1/2} \equiv \mathcal{A}$$

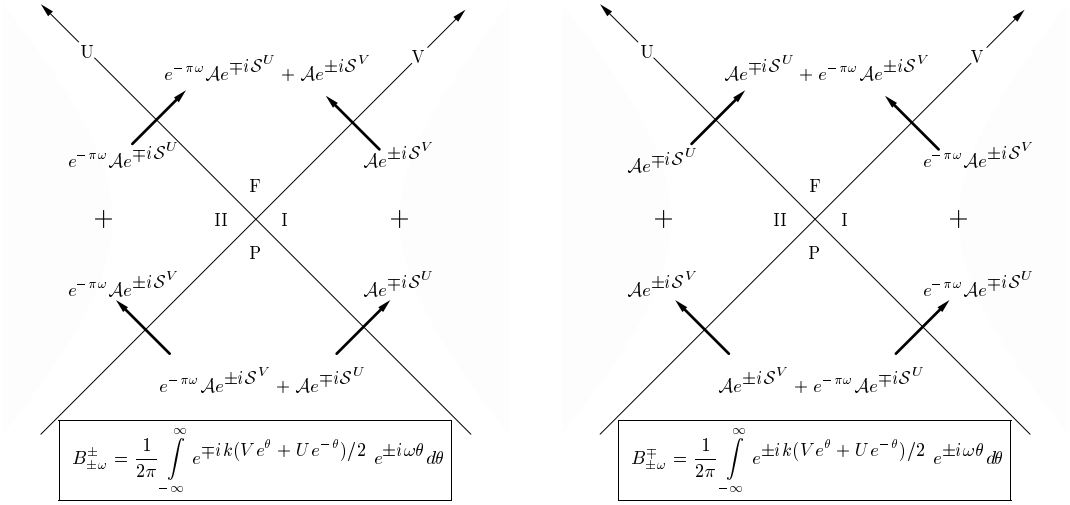

FIG. 7. WKB-approximate formulas for the Minkowski-Bessel modes. All formulas assume that $\omega = |\omega|$. The upper (lower) signs in a picture go only with the upper (lower) signs in the corresponding boxed formula. This means, for example, that the formula (in all four Rindler sectors) for a M-B of, say, positive Minkowski frequency and of negative Rindler frequency, is designated by $B^{+}_{-\omega}$, and is given by the lower signed expressions in the second picture. The complete propagation process (splitting, reflection, and interference) of a M-B mode is characterized by the phase $\mathcal{S}^U$, which is continuous across the U-axis, and the phase $\mathcal{S}^V$, which is continuous across the V-axis. Both satisfy the Hamilton-Jacobi equation $\frac{\partial S}{\partial U}\frac{\partial S}{\partial V} = -\frac{k^2}{4}$, which is implied by Eq.(5). The amplitude $\mathcal{A}$ or $(e^{-\pi\omega}\mathcal{A})$ of each WKB wave propagating across its respective event horizon satisfies the concomitant conservation law $\frac{\partial}{\partial U}\left(\mathcal{A}^2\frac{\partial S}{\partial V}\right) + \frac{\partial}{\partial V}\left(\mathcal{A}^2\frac{\partial S}{\partial U}\right) = 0$, where $S = \mathcal{S}^U$ or $\mathcal{S}^V$, depending on which horizon is being crossed.

A. Space of Test Functions

Recall that, unlike ordinary functions, generalized functions are not defined by themselves, but depend on the space of test functions. This means that a generalized function is a linear functional on the space of test functions. The space of test functions can be one of several possibilities, but the one we are mainly interested in consists of those functions *which are the Fourier transforms of functions compact support*. The formula for such test functions is

$$\hat{\phi}(\omega) = \frac{1}{\sqrt{2\pi}}\int_{-\infty}^{\infty} \phi(\theta) e^{i\omega\theta} d\theta$$
$$= \frac{1}{\sqrt{2\pi}}\int_{-a}^{a} \phi(\theta) e^{i\omega\theta} d\theta$$

because the support of $\phi(\theta)$ is confined to the compact region $|\theta| \le a$. These test functions, $\hat{\phi}(\omega)$, are entire analytic functions of their argument $z = \omega + i\zeta$, and they satisfy the inequality

$$|\hat{\phi}(\omega + i\zeta)| \le Ce^{a|\zeta|} \quad . \tag{16}$$

Adapting the notation of Gelfand and Shilov [8], we shall call the space of such test functions Z_0. This is the space of test functions whose inverse Fourier transforms, the space K_0, are of compact support. Thus ϕ belongs to K_0, while the Fourier transform of ϕ, the test function $\hat{\phi}$, belongs to Z_0. The subscript zero designates the fact that each ϕ is piecewise continuous, while Z_1 would be the space of Fourier transforms of continuous functions with compact support, Z_2 the space of Fourier transforms of functions with continuous first derivatives and with compact support, etc., and $Z_\infty \equiv Z$ the Fourier transform of $K_\infty \equiv K$, the space of infinitely differentiable ("smooth") functions with compact support.

B. Spacetime-Parametrized Family of Generalized Functions

Generalized functions fall into two mutually exclusive and jointly exhaustive types: *regular* and *singular*. We shall need to consider both.

A *regular* generalized function is a linear functional on Z_0 defined by the integral of an ordinary (and locally integrable) function multiplied by a test function in Z_0.

Accelerated frames give rise to two regular (U,V)-parametrized families of generalized functions. They are defined by the linear functional (asterisk * denotes complex conjugate)

$$\int_{-\infty}^{\infty} \hat{\phi}(\omega)^* \; B_\omega^\pm(kU,kV)\; d\omega \equiv (\hat{\phi}, B^\pm(kU,kV)) \tag{17}$$

on the test functions $\hat{\phi}(\omega)$, which belong to Z_0. The function $B_\omega^\pm(kU,kV)$ is represented by the integral Eq.(12), which is an ordinary function of ω whenever (U,V) lies in the interior of the four Rindler sectors I, II, P, or F.

Notational Remark. Even though there are *two* families, *two* integrals, *two* generalized functions, and so on, we shall from now on refer to the two collectively in the singular, and not in the plural, and let the plus and minus sign serve as labels that refer to one or the other.

The integral representatives for $B_\omega^\pm(kU,kV)$ are exhibited in Figures 4a and 4b for each of the four Rindler sectors. The requisite relation between the Rindler coordinates (τ,ξ) and the null coordinates (U,V) in these four Rindler Sectors is shown in Figure 1.

The space of all linear functionals on Z_0 forms a linear space in its own right, and its name is Z_0'. The set of regular generalized functions

$$\{B^\pm(kU,kV):\ (U,V) \text{ lies inside one of the Rindler Sectors}\} \tag{18}$$

is a subset of Z_0'. More precisely, let

$$R = I \cup II \cup P \cup F \tag{19}$$

be the union of the interior of the four Rindler quadrants. Then the two-parameter family $B^\pm(kU,kV)$ is a continuous map from R into Z_0', the space of all generalized functions associated to Z_0:

$$B^\pm \;:\; R \;\longrightarrow\; Z_0' \quad . \tag{20}$$

In fact, the map is a smooth map because all its derivatives with respect to U and V exist in its whole domain, $I \cup II \cup P \cup F$

However, when (U,V) approaches the event horizon, a point on the boundary of R, then the (U,V)-parametrized *ordinary* function $B_\omega^\pm(kU,kV)$ does not tend towards an ordinary function. In fact, the limit does not even exist. Nevertheless, we shall see that the integral, Eq.(17), does tend towards a limit for all test functions in Z_0. Thus the generalized function $B^\pm(kU,kV)$ has a limit as (U,V) approaches the event horizon, even though the ordinary function $B_\omega^\pm(kU,kV)$ does not.

C. Extension Onto the Event Horizon

Each of the null coordinates U and V is smooth across the event horizon. However, the (U,V)-parametrized family of generalized functions $B^\pm(kU,kV)$ is not, because it is not even defined there. What we need is an *extension* of this family across the event horizon. This means that this extended two-parameter family, call it $\overline{B}^\pm(kU,kV)$, is the same as the original family $B^\pm(kU,kV)$, except that the parameter domain of $\overline{B}^\pm(kU,kV)$ is bigger than that of $B^\pm(kU,kV)$.

1. Definition

The parameter domain of the to-be-constructed extension should be *all* of Minkowski spacetime,

$$\overline{R} = \; I \cup II \cup P \cup F \cup \{(U,V) : UV = 0\} \quad , \tag{21}$$

which includes also the event horizons

$$\{(U,V):\ UV=0\} \quad , \tag{22}$$

the boundary of the four Rindler Sectors I, II, P, and F. Thus the to-be-constructed extension is a map from $\overline{R}$ into Z_0',

$$\overline{B}^{\pm} \ : \ \overline{R} \ \longrightarrow \ Z_0' \quad . \tag{23}$$

with the property that

$$\overline{B}^{\pm}(kU,kV) = B^{\pm}(kU,kV) \quad \text{whenever} \ \ (U,V)\in R \quad ; \tag{24}$$

that is $\overline{B}^{\pm}|_R = B^{\pm}$.

A map, such as Eq.(23), is said to be an *extension* of the map Eq.(20), because $R\subset\overline{R}$ and $\overline{B}^{\pm}|_R = B^{\pm}$.

An extension of the two-parameter family $B^{\pm}(kU,kV)$, Eq.(17), to the event horizons, Eq.(22), is not arbitrary. In fact, it is (i) unique, (ii) continuous, and (iii) even smooth. This, we shall see, is because this extension is related by the Fourier transform to the Minkowski plane wave amplitude on the mass hyperbola, Eqs.(7), (8). This amplitude, Eq.(6), is a (U,V)-parametrized family of ordinary functions. Its parameter domain includes all of spacetime, including the event horizons, Eq.(22). This fact is the key to $\overline{B}^{\pm}(kU,kV)$, the continuous and smooth extension of $B^{\pm}(kU,kV)$.

2. Construction

The construction of $\overline{B}^{\pm}(kU,kV)$ is based on a familiar idea, namely, Parceval's theorem. Let us fix notation by letting

$$\hat{\phi}(\omega) = \frac{1}{\sqrt{2\pi}}\int_{-\infty}^{\infty}\phi(\theta)e^{i\omega\theta}d\theta \tag{25}$$
$$\hat{f}(\omega) = \frac{1}{\sqrt{2\pi}}\int_{-\infty}^{\infty}f(\theta)e^{i\omega\theta}d\theta$$

be the Fourier transforms of ϕ and f. Then, with the asterisk, *, denoting complex conjugate, one has

$$\begin{aligned}(\phi,f) &\equiv \int_{-\infty}^{\infty}\phi(\theta)^* f(\theta)\ d\theta = \int_{-\infty}^{\infty}\phi(\theta)^*\left\{\frac{1}{\sqrt{2\pi}}\int_{-\infty}^{\infty}\hat{f}(\omega)e^{-i\omega\theta}d\omega\right\}d\theta \\ &= \int_{-\infty}^{\infty}\hat{f}(\omega)\left\{\frac{1}{\sqrt{2\pi}}\int_{-\infty}^{\infty}\phi(\omega)e^{i\omega\theta}d\theta\right\}^* d\omega = \int_{-\infty}^{\infty}\hat{\phi}(\omega)^*\hat{f}(\omega)\ d\omega \\ &= (\hat{\phi},\hat{f}) \quad .\end{aligned}$$

This is Parceval's theorem. We now turn this theorem around and use its conclusion,

$$(\hat{\phi},\hat{f}) = (\phi,f)\ , \tag{26}$$

to define the generalized function $\hat{f}$. Its domain is the space Z_0 of test functions $\hat{\phi}(\omega)$. For a given function f, the value of this linear functional $\hat{f}$ is uniquely determined by the integral on the right hand side. This is because $\phi(\theta)$ belongs to K_0, the space of functions with compact support $-a\le\theta\le a$.

Apply this "inverted Parceval's theorem" to the function

$$f(\theta) = \frac{1}{\sqrt{2\pi}}e^{\mp ik(Ve^{\theta}+Ue^{-\theta})/2}\ ,$$

the plane wave amplitude, Eq.(6). Denote the resulting linear functional by

$$\hat{f} = \overline{B}^{\pm}(kU, kV) \ .$$

One, therefore, has the following definition

$$(\hat{\phi}, \overline{B}^{\pm}(kU, kV)) \equiv \int_{-\infty}^{\infty} \phi(\theta)^* \left(\frac{1}{\sqrt{2\pi}} e^{\mp ik(Ve^{\theta} + Ue^{-\theta})/2} \right) d\theta \quad . \tag{27}$$

This integral (as well as all its partial derivatives with respect to U and V) is obviously finite because $\phi(\theta)$ has compact support. In fact, this integral, as well as all its derivatives, are finite for all parameter values $-\infty < U, V < \infty$, even for those for which $UV = 0$. Furthermore, for every $\hat{\phi}(\omega)$ in Z_0, this integral depends continuously and smoothly on the parameter pair (U, V). Consequently, the generalized function $\overline{B}^{\pm}(kU, kV)$ defined by Eqs.(25,27) is a continuous and smooth function of the parameters U and V, including those (U, V) which lie on the event horizon.

The usefulness of $\overline{B}^{\pm}(kU, kV)$ as defined by Eqs.(25,27) derives from the fact that it coincides with $B^{\pm}(kU, kV)$, Eq.(12), whenever (U, V) lies in R, Eq.(19). If true, this makes $\overline{B}^{\pm}$ the extension of $B^{\pm}$. This is verified below. In the next section (Section V) we shall see how this coincidence leads to a very intuitive integral representation of $\overline{B}^{\pm}(kU, kV)$.

Consider $\overline{B}^{\pm}(kU, kV)$ as defined by Eqs.(25,27). The fact that $\phi(\theta)$ is of compact support, say $-a < \theta < a$, yields

$$\begin{aligned}
(\hat{\phi}, \overline{B}^{\pm}(kU, kV)) &\equiv \int_{-\infty}^{\infty} \phi(\theta)^* \frac{1}{\sqrt{2\pi}} e^{\mp ik(Ve^{\theta} + Ue^{-\theta})/2} d\theta \\
&= \int_{-a}^{a} \phi(\theta)^* \frac{1}{\sqrt{2\pi}} e^{\mp ik(Ve^{\theta} + Ue^{-\theta})/2} d\theta \\
&= \int_{-\infty}^{\infty} \hat{\phi}(\omega)^* \left[\frac{1}{2\pi} \int_{-a}^{a} e^{\mp ik(Ve^{\theta} + Ue^{-\theta})/2} e^{i\omega\theta} d\theta \right] d\omega \quad .
\end{aligned} \tag{28}$$

This double integral is unchanged if one lets $a \to \infty$. Consequently, for $UV \neq 0$ the θ-integral has the limit

$$\lim_{a \to \infty} \ \frac{1}{2\pi} \int_{-a}^{a} e^{\mp ik(Ve^{\theta} + Ue^{-\theta})/2} e^{i\omega\theta} d\theta \equiv B^{\pm}_{\omega}(kU, kV) \quad , \tag{29}$$

whose value $B^{\pm}_{\omega}(kU, kV)$ inside any one of the Rindler Sectors is indicated in Figures 4a and 4b. Thus, Eq.(28) becomes

$$\begin{aligned}
(\hat{\phi}, \overline{B}^{\pm}(kU, kV)) &= \int_{-\infty}^{\infty} \hat{\phi}(\omega)^* B^{\pm}_{\omega}(kU, kV) \ d\omega \equiv \\
&\equiv (\hat{\phi}, B^{\pm}(kU, kV)) \quad .
\end{aligned} \tag{30}$$

This holds for all test functions $\hat{\phi}$. Consequently, we have

$$\overline{B}^{\pm}(kU, kV) = B^{\pm}(kU, kV) \quad \text{whenever} \quad (U, V) \in R \quad ;$$

that is $\overline{B}^{\pm}|_R = B^{\pm}$. In other words, $\overline{B}^{\pm}(kU, kV)$ *is an extension of* $B^{\pm}(kU, kV)$ indeed.

3. Smoothness

It is clear that the extension $\overline{B}^{\pm}(kU, kV)$ is continuous and smooth in the parameters U and V when (U, V) lies in the interior of one of the Rindler Sectors; after all, there, by construction, $\overline{B}^{\pm}$ coincides with $B^{\pm}$, which is continuous and smooth in U and V. But $\overline{B}^{\pm}(kU, kV)$ is also continuous and smooth when (U, V) lies on the boundary, Eq.(22). For example, continuity of $\overline{B}^{\pm}$ is expressed by

$$\lim_{(U,V)\to(U_0,V_0)} \overline{B}^{\pm}(kU,kV) = \overline{B}^{\pm}(kU_0,kV_0) \quad , \tag{31}$$

while smoothness is expressed by

$$\lim_{(U,V)\to(U_0,V_0)} \quad \frac{\partial^{m+n}}{\partial U^m \partial V^n}\overline{B}^{\pm}(kU,kV) = \frac{\partial^{m+n}}{\partial U^m \partial V^n}\overline{B}^{\pm}(kU_0,kV_0) \tag{32}$$

This is obtained by differentiating Eq.(28)

$$\left(\hat{\phi}, \frac{\partial^{m+n}}{\partial U^m \partial V^n}\overline{B}^{\pm}(kU,kV)\right) \tag{33}$$

$$\equiv \left(\mp\frac{ik}{2}\right)^{m+n} \int_{-\infty}^{\infty} \phi(\theta)^* \left[\frac{1}{\sqrt{2\pi}} e^{\mp ik(Ve^{\theta}+Ue^{-\theta})/2} e^{(n-m)\theta}\right] d\theta \tag{34}$$

$$= \left(\mp\frac{ik}{2}\right)^{m+n} \int_{-a}^{a} \phi(\theta)^* \left[\frac{1}{\sqrt{2\pi}} e^{\mp ik(Ve^{\theta}+Ue^{-\theta})/2} e^{(n-m)\theta}\right] d\theta \tag{35}$$

$$= \left(\mp\frac{ik}{2}\right)^{m+n} \int_{-\infty}^{\infty} \hat{\phi}(\omega)^* \left[\frac{1}{2\pi} \int_{-a}^{a} e^{\mp ik(Ve^{\theta}+Ue^{-\theta})/2} e^{(n-m)\theta} e^{i\omega\theta} d\theta\right] d\omega \quad .$$

This expression depends continuously on the parameter pair (U,V), even when (U,V) lies on one of the event horizons where $UV=0$. This is guaranteed by the finiteness of the the integral in Eq.(35). Consequently, one has

$$\lim_{(U,V)\to(U_0,V_0)} \quad \left(\hat{\phi}, \frac{\partial^{m+n}}{\partial U^m \partial V^n}\overline{B}^{\pm}(kU,kV)\right) = \left(\hat{\phi}, \frac{\partial^{m+n}}{\partial U^m \partial V^n}\overline{B}^{\pm}(kU_0,kV_0)\right) \quad . \tag{36}$$

This holds for all test functions $\hat{\phi}(\omega)$ belonging to Z_0, and thus verifies the smoothness condition (32) at all events (U_0,V_0) of Minkowski spacetime.

D. Other Test Function Spaces

This smoothness raises two pertinent questions: Are there any other test function spaces, besides Z_0, relative to which $\overline{B}^{\pm}(kU,kV)$ depends continuously on the parameters U and V? and: What are these test function spaces good for?

We answer the last question first by noting that these spaces supply us with complete sets of orthonormal basis functions which are square-integrable on the real line. They are exhibited for the first two examples below. From these sets one obtains quite trivially complete sets of Klein-Gordon-orthonormal wavepacket histories, the dynamical degrees of freedom of the Klein-Gordon system. Their construction is illustrated in Section VII.

The answer to the first question is "yes", there are other test function spaces. What are they? That depends entirely on the behavior which $\overline{B}^{\pm}(kU,kV)$ is required to have. This means that one talks about *the properties* of the generalized function $\overline{B}^{\pm}(kU,kV)$ *relative to the given space of test functions.*

1.) As a first example, consider Z_0 as was done above. One says that $\overline{B}^{\pm}(kU,kV)$ is smooth (i.e. infinitely differentiable) *relative to the given space of test functions* Z_0. The functions of this space are very useful because they and their Fourier transforms accommodate orthonormal bases which, as shown in Section VII.B, lead to sets (i.e. bases) of Klein-Gordon-orthonormal wave packet histories.

However, a cursory examination of these wave packet solutions shows that they are based on orthonormal test functions whose Fourier transform is discontinuous on the θ-domain, the mass hyperboloid Eqs.(7), (8). To ward off such a potentially unphysical assumption, we shall exhibit a set of test functions whose Fourier transform is smooth on the θ-domain, *and* relative to which the Minkowski-Bessel distribution yields wave packet histories which are still smooth everywhere, including the event horizons. We shall do this in the next example.

2.) As a second example, consider the space of smooth test functions which decay faster than any exponential. We shall denote this space by G because it accommodates the set of functions with Gaussian decay,

$$\phi(\theta) = H_n(\theta)e^{-\theta^2/2} \quad , \qquad n = 0,1,2,\cdots \quad , \tag{37}$$

where $H_n(\theta)$ is the Hermite polynomial of order n. These Gaussian test functions ("simple harmonic oscillator eigenfunctions") have the delightful property that they are eigenfunctions of the unitary Fourier transform:

$$\int_{-\infty}^{\infty} e^{-\theta^2/2} H_n(\theta) \frac{e^{i\omega\theta}}{\sqrt{2\pi}}\, d\theta = i^n\ e^{-\omega^2/2} H_n(\omega)\ . \tag{38}$$

The eigenfunction property of these Gaussian test functions secures the best of both worlds: (1) faster than exponential decay on the Minkowski frequency θ-parameter domain *and* (2) smoothness both on the Rindler frequency (ω) domain and the Minkowski frequency θ-domain.

Thus we have achieved our goal of exhibiting a set of test functions which together with their Fourier transforms are smooth *and* which guarantee the convergence of the integral, Eq.(34), and hence guarantee the continuity of all spacetime derivatives, Eq.(32), of the Minkowski-Bessel distribution.

3.) As a third, but less important example, consider the space K_0 consisting of test functions $\hat{\psi}(\omega)$ with compact support on the Rindler frequency line $-\infty < \omega < \infty$. This test function space is very different from Z_0 of example 1. In fact, with Z_0 consisting only of entire analytic functions, these two spaces have no common element except the zero function. (A non-zero function of compact support cannot be analytic.) It is quite easy to see that, relative to the test function space K_0, the extension $\overline{B}^{\pm}(kU, kV)$ is continuous (but not smooth) in the parameters U and V. Indeed, consider the (inverse) Fourier transform

$$\psi(\theta) = \frac{1}{\sqrt{2\pi}} \int_{-\infty}^{\infty} \hat{\psi}(\omega) e^{-i\omega\theta} d\omega \tag{39}$$

of $\hat{\psi}(\omega)$, which is a function of compact support. This (inverse) Fourier transform is a function which decays at least as rapidly as $\frac{1}{|\theta|}$ along the θ-axis. Consequently,

$$\begin{aligned} (\hat{\psi}, \overline{B}^{\pm}(kU, kV)) &= \int_{-\infty}^{\infty} \hat{\psi}(\omega)^* B^{\pm}_{\omega}(kU, kV)\ d\omega \\ &\equiv \int_{-\infty}^{\infty} \psi(\theta)^* \frac{1}{\sqrt{2\pi}} e^{\mp ik(Ve^{\theta} + Ue^{-\theta})/2} d\theta \end{aligned} \tag{40}$$

is a convergent integral which depends continuously on the parameters U and V. Thus one says that $\overline{B}^{\pm}(kU, kV)$ is continuous also *relative* to the space of smooth test functions of compact support. However, it is obviously not smooth relative to this space of test functions.

V. THE GLOBAL REPRESENTATION

Let us summarize the construction of the two families of generalized functions $B^{+}(kU, kV)$ and $B^{-}(kU, kV)$, including their unique extensions onto the event horizon:

Consider the Fourier transform representation of the boost-invariant Cauchy evolution, Eq.(12),

$$B^{\pm}_{\omega}(kU, kV) = \lim_{a\to\infty} \frac{1}{2\pi} \int_{-a}^{a} e^{\mp ik(Ve^{\theta} + Ue^{-\theta})/2} e^{i\omega\theta} d\theta \quad . \tag{41}$$

This integral is always well-defined, provided one remembers to include into its definition the requirement that one take the limit *after* one has done the requisite ω-integration,

$$\int_{-\infty}^{\infty} \hat{\phi}(\omega)^* B^{\pm}_{\omega}(kU, kV)\ d\omega = \tag{42}$$

$$= \lim_{a\to\infty} \int_{-\infty}^{\infty} \hat{\phi}(\omega)^* \left[\frac{1}{2\pi} \int_{-a}^{a} e^{\mp ik(Ve^{\theta} + Ue^{-\theta})/2} e^{i\omega\theta} d\theta \right]\ d\omega \quad . \tag{43}$$

(Here, as in example 1 of Section IV.D, one can take $\hat{\phi}(\omega) \in Z_0$, i.e. is any test function whose Fourier transform has compact support in the θ-domain)

If one keeps this rule in mind, then Eq.(41) coincides with the shorthand formula, Eq.(12),

$$B^{\pm}_{\omega}(kU, kV) = \frac{1}{2\pi} \int_{-\infty}^{\infty} e^{\mp ik(Ve^{\theta} + Ue^{-\theta})/2} e^{i\omega\theta} d\theta \quad , \tag{44}$$

not only whenever (U, V) lies in the interior of any of the four Rindler sectors, but also whenever $UV = 0$, i.e. when (U, V) lies on any one of the event horizons.

As a point of curiosity, we note that in the first case, when $UV \neq 0$, $B^{\pm}(kU, kV)$ is a *regular* distribution, which means that the integral in Eq.(44) converges to an ordinary function of ω. In the second case, when $UV = 0$, $B^{\pm}(kU, kV)$ is a *singular* distribution, which means that the integral in Eq.(44) does not converge to an ordinary function of ω. In that case one must resort to Eq.(43) in order to impart meaning to Eq.(44)

VI. QUANTUM MECHANICAL TUTORIAL: DISTRIBUTIONS AS SUMS OVER INTERFERING ALTERNATIVES

The (U, V)-parametrized family of distributions $B^{\pm}_{\omega}(kU, kV)$ constitutes a flexible supply for the constructing other physically important distributions. The transition amplitude of an accelerated quantum system ("detector") is a key example. Within first order perturbation theory this amplitude, we recall, is a linear superposition, in fact a spacetime integral, over that set of events (U, V) where the interaction between the detector and the ambient field is non-zero. The resultant superposition ("sum over interfering alternatives") is a new distribution, the transition amplitude.

Of particular significance is the amplitude for the detector to make a transition and thereby create a photon from the Minkowski vacuum. This amplitude, which is based on the interaction action

$$S_{int} = \int_{-\infty}^{\infty} \psi(x^{\mu}(\tau))\ m(\tau)c(\tau)\ d\tau \quad , \tag{45}$$

is

$$\begin{aligned} A^{Mink}(\omega, \tau) &= {}_M\langle 1_{\omega}| \otimes \langle E_{fin}|\ \psi(x^{\mu}(\tau))\ m(\tau)c(\tau)\ |0\rangle_M \otimes |E_{init}\rangle \\ &= {}_M\langle 1_{\omega}|\psi(x^{\mu}(\tau))|0\rangle_M\ \langle E_{fin}|m(\tau)c(\tau)|E_{init}\rangle \quad . \end{aligned} \tag{46}$$

Here

$$\{x^{\mu}(\tau)\} = \{U(\tau), V(\tau) : \ -\infty < \tau < \infty\}$$

is the detector world line. The field is

$$\psi(x^{\mu}) = \int_{-\infty}^{\infty} \{a_{\omega} B^{+}_{\omega}(kU, kV) + a^{*}_{\omega} \left[B^{+}_{\omega}(kU, kV)\right]^{*}\}\ d\omega \quad . \tag{47}$$

The detector is coupled to this field by means of its dynamical property

$$m(\tau) = e^{iH_0\tau} m(0) e^{-iH_0\tau} \tag{48}$$

whose evolution is controlled by the detector Hamiltonian H_0. The scalar $c(\tau)$ is a time-dependent coupling constant, a square integrable function, which expresses the finite time interval, say $-T \leq \tau \leq T$, during which the detector interacts with the field. For the sake of concreteness one may assume that this coupling function decays exponentially outside this interval. Thus one can take $c(\tau)$ to be

$$c(\tau) = c_0 \begin{cases} e^{\alpha(\tau+T)} & \tau < -T \\ 1 & -T \leq \tau \leq T \\ e^{-\alpha(\tau-T)} & T < \tau \end{cases} \tag{49}$$

Note that this function is continuous, but that it becomes discontinuous in the limit $\alpha \to \infty$.

A. Interfering and Exclusive Alternatives

We say that the expression $A^{Mink}(\omega,\tau)$ is the amplitude for finding the interacting detector-field system in the state ${}_M\langle 1_\omega| \otimes \langle E_{fin}\ |$ if, as a result of the interaction at event $\{x^\mu(\tau)\}$, the system is in the state $|\psi(x^\mu(\tau))|0\rangle_M \otimes |m(\tau)c(\tau)|E_{init}\rangle$.

Thus, for each event along the detector's world line, there is a unique amplitude, Eq.(46), that (i) the detector has made a transition to the state $\langle E_{fin}|$ and that (ii) a Minkowski photon of Rindler frequency ω $(-\infty<\omega<\infty)$ has been created from the Minkowski vacuum state. This amplitude, Eq.(46), is a distribution for each value of τ, and it is given with the help of Eqs.(47) and (48) by

$$A^{Mink}(\omega,\tau)=\langle E_{fin}|m(0)|E_{init}\rangle e^{iE_{fin}\tau}c(\tau)\left[B^+_\omega(kU(\tau),kV(\tau))\right]^* e^{-iE_{init}\tau}$$

The total amplitude is obtained by summing over all these interfering alternatives labeled by the events $(-\infty<\tau<\infty)$ on the detector world line:

$$\begin{aligned}\int_{-\infty}^{\infty} A^{Mink}(\omega,\tau)\ d\tau &= {}_M\langle 1_\omega| \otimes \langle E_{fin}\ |S_{int}\ |0\rangle_M \otimes |E_{init}\rangle \\ &= \langle E_{fin}|m(0)|E_{init}\rangle \int_{-\infty}^{\infty} e^{iE_{fin}\tau}c(\tau)\left[B^+_\omega(kU(\tau),kV(\tau))\right]^* e^{-iE_{init}\tau}\ d\tau \\ &\equiv A^{Mink\ Emit}(\omega)\quad . \end{aligned} \tag{50}$$

This is another distribution, the complex amplitude that the detector make a transition to the state $\langle E_{fin}|$ while simultaneously creating a Minkowski photon of Rindler frequency ω $(-\infty<\omega<\infty)$ during the time interval imposed by the function $c(\tau)$. The following two points need to be reemphasized:

1. The totalized transition amplitude $A^{Mink\ Emit}(\omega)$ is quite general: no assumptions about the detector world line have been made as yet.

2. This amplitude is for the emission of a Minkowski photon whose *moment of energy* [9] relative to the reference event (t_0,z_0) is ω $(-\infty<\omega<\infty)$. Even though we have been referring to this quantity as the "Rindler frequency" of a Minkowski photon, one should not confuse this property with the "Rindler frequency" of a Rindler-Fulling quantum. The first generates Lorentz boosts in all of Minkowski spacetime, while the second generates Rindler time translations in Rindler Sector I (or II) only.

The emission of Minkowski photons having this, that, or the other Rindler frequency ω $(-\infty<\omega<\infty)$ when the detector makes a transition are not *interfering alternatives*, but instead are *exclusive alternatives* [10]. This is why the unconditional detector transition probability is the sum, or more precisely the integral, of the *squared* modulus of $A^{Mink\ Emit}(\omega)$, the probability amplitude:

$$\int_{-\infty}^{\infty} |A^{Mink\ Emit}(\omega)|^2\ d\omega\quad . \tag{51}$$

This unconditional transition probability is the total probability for the detector to make a transition as predicted by first order perturbation theory based on Eq.(45).

Quantum mechanics tells us that $|A^{Mink\ Emit}(\omega)|^2\ d\omega$ is the differential detector transition probability conditioned by the emission of a Minkowski photon of type ω $(-\infty<\omega<\infty)$. Consequently, nature demands that the amplitude $A^{Mink\ Emit}(\omega)$ be a very special type of distribution, namely a square-integrable function of ω. Thus our formulation must satisfy

$$\int_{-\infty}^{\infty} |A^{Mink\ Emit}(\omega)|^2\ d\omega \equiv \mathcal{P}^{Mink\ Emit}<\infty\quad . \tag{52}$$

Higuchi, Matsas, and Peres [11] (HMP) have shown that this is indeed the case if and only if the detector is switched on and off in a continuous way (i.e. if and only if $c(\tau)$ depends continuously on τ) whenever it undergoes uniform acceleration in Rindler Sector I.

B. Relations Among Transition Amplitudes and Probabilities

Let us assume, therefore, that the interaction of the uniformly accelerated detector is confined to that portion of its history which lies strictly in Rindler Sector I. In that case the amplitude $A^{Mink\ Emit}(\omega)$, Eq.(50), is a regular distribution, an ordinary function of ω whose form for $\omega > 0$ is

$$\begin{aligned} A^{Mink\ Emit}(\omega) &= \langle E_{fin}|m(0)|E_{init}\rangle \int_{-\infty}^{\infty} e^{iE_{fin}\tau} c(\tau) \left[\frac{\sqrt{2\sinh\pi\omega}}{\pi} K_{i\omega}(k\xi) e^{-i\omega\tau} \right]^* \frac{e^{\pi\omega/2}}{\sqrt{2\sinh\pi\omega}} e^{-iE_{init}\tau}\, d\tau \\ &= \langle E_{fin}|m(0)|E_{init}\rangle \int_{-\infty}^{\infty} e^{iE_{fin}\tau} c(\tau)\ {}_R\langle 1_\omega|\ \psi(x^\mu(\tau))\ |0\rangle_R\ \ e^{-iE_{init}\tau}\, d\tau \left(1 + \frac{1}{\exp 2\pi\omega - 1}\right)^{1/2} \\ &\equiv A^{Rind\ Emit}(\omega) \left(1 + \frac{1}{\exp 2\pi\omega - 1}\right)^{1/2} \qquad\qquad 0 < \omega \end{aligned} \tag{53}$$

Here $A^{Rind\ Emit}(\omega)$ is the amplitude for the process of the detector making the transition $|E_{init}\rangle \to |E_{fin}\rangle$ while emitting a Fulling-Rindler quantum of Rindler frequency $\omega > 0$ into the Fulling-Rindler vacuum $|0\rangle_R$. One is forced into this identification of $A^{Rind\ Emit}(\omega)$ because the normal mode expansion of the Klein-Gordon field in Rindler Sector I is

$$\psi(x^\mu) = \int_0^\infty \{A_\omega \frac{\sqrt{2\sinh\pi\omega}}{\pi} K_{i\omega}(k\xi) e^{-i\omega\tau} \quad + A_\omega^* \frac{\sqrt{2\sinh\pi\omega}}{\pi} K_{i\omega}(k\xi) e^{i\omega\tau}\ \}\, d\omega$$

with

$$A_\omega|0\rangle_R = 0 \quad .$$

However, when $\omega = -|\omega| < 0$, the amplitude $A^{Mink\ Emit}(\omega)$ leads to a different quantity:

$$\begin{aligned} A^{Mink\ Emit}(-|\omega|) &= \langle E_{fin}|m(0)|E_{init}\rangle \int_{-\infty}^{\infty} e^{iE_{fin}\tau} c(\tau) \left[\frac{\sqrt{2\sinh\pi|\omega|}}{\pi} K_{i\omega}(k\xi) e^{i|\omega|\tau} \right]^* \frac{e^{-\pi|\omega|/2}}{\sqrt{2\sinh\pi|\omega|}} e^{-iE_{init}\tau}\, d\tau \\ &= \langle E_{fin}|m(0)|E_{init}\rangle \int_{-\infty}^{\infty} e^{iE_{fin}\tau} c(\tau)\ {}_R\langle 0|\ \psi(x^\mu(\tau))\ |1_{|\omega|}\rangle_R\ \ e^{-iE_{init}\tau}\, d\tau \left(\frac{1}{\exp 2\pi|\omega| - 1}\right)^{1/2} \\ &\equiv A^{Rind\ Abs}(|\omega|) \left(\frac{1}{\exp 2\pi|\omega| - 1}\right)^{1/2} \qquad\qquad \omega < 0 \end{aligned} \tag{54}$$

In this case $A^{Rind\ Abs}(|\omega|)$ is the amplitude for the process of the detector making the same transition $|E_{init}\rangle \to |E_{fin}\rangle$, but this time absorbing a Fulling-Rindler quantum (of frequency $|\omega| = -\omega > 0$) and leaving the field in the Fulling-Rindler vacuum $|0\rangle_R$. The relationships, Eqs.(53) and (54), between the probability amplitudes imply that

$$\int_{-\infty}^{\infty} |A^{Mink\ Emit}(\omega)|^2\, d\omega = \int_0^\infty |A^{Rind\ Emit}(\omega)|^2 \left(1 + \frac{1}{\exp 2\pi\omega - 1}\right) d\omega + \int_0^\infty |A^{Rind\ Abs}(\omega)|^2 \left(\frac{1}{\exp 2\pi\omega - 1}\right) d\omega \quad , \tag{55}$$

or more compactly

$$\mathcal{P}^{Mink\ Emit} = \mathcal{P}^{Rind\ Emit} + \mathcal{P}^{Rind\ Abs} \quad . \tag{56}$$

This equation relates the detector transition probability when a Minkowski photon is emitted to the transition probability when a Fulling-Rindler quantum is emitted *or* absorbed.

C. Finite-time Detector

What is of particular interest, is how these probabilities depend on (i) the time duration, $2T$, of the interaction strength, Eq.(49), between the detector and the ambient field, (ii) the detector's switching time $\frac{1}{\alpha}$, and (iii) the detector's transition energy $\Delta E = E_{fin} - E_{init}$. Quantum mechanics answers these questions by furnishing us with explicit expressions for the three probability amplitudes,

$$A^{Mink\ Emit}(\omega) = \langle E_{fin}|m(0)|E_{init}\rangle f(\omega - \Delta E)\frac{e^{\pi\omega/2}}{\pi}K_{i\omega}(k\xi) \qquad -\infty < \omega < \infty \tag{57}$$

$$A^{\begin{matrix}Rind\\ \ \end{matrix}\ \begin{matrix}Emit\\ Abs\end{matrix}}(\omega) = \langle E_{fin}|m(0)|E_{init}\rangle f(\omega \mp \Delta E)\frac{\sqrt{2\sinh\pi\omega}}{\pi}K_{i\omega}(k\xi) \qquad 0 < \omega < \infty \quad , \tag{58}$$

where the function

$$\begin{aligned} f(\omega \mp \Delta E) &\equiv \int_{-\infty}^{\infty} e^{iE_{fin}\tau}c(\tau)e^{\mp i\omega\tau}e^{-iE_{init}\tau}\,d\tau \\ &= \frac{2\alpha}{\alpha^2 + (\omega \mp \Delta E)^2}\cos T(\omega \mp \Delta E) + 2\left(\frac{1}{\omega \mp \Delta E} - \frac{\omega \mp \Delta E}{\alpha^2 + (\omega \mp \Delta E)^2} + \right)\sin T(\omega \mp \Delta E) \end{aligned} \tag{59}$$

is a temporal overlap integral. It is an even function of its argument, and it expresses the resonance between the Rindler field oscillator $e^{\mp i\omega\tau}$ and the transition frequency ($E_{fin} - E_{init} = \Delta E$) oscillator $e^{-i\Delta E\tau}$ of the detector.

By introducing the probability amplitudes $A^{Rind\ Emit}$ and $A^{Rind\ Abs}$ into Eq.(56), which HMP infer from Unruh's original work, they show that probability is finite, i.e.

$$\mathcal{P}^{Rind\ Emit} + \mathcal{P}^{Rind\ Abs} = \mathcal{P}^{Mink\ Emit} < \infty \quad , \tag{60}$$

if and only if the function $c(\tau)$ is continuous, i.e. the switching time $\frac{1}{\alpha}$ is non-zero. Using their result we conclude from this that, under these conditions, the amplitude $A^{Mink\ Emit}$, Eq.(57) is a distribution which is a square-integrable function of ω.

The physical significance of HMP's finiteness result is that the total probability in Eq.(60) complies with Fermi's golden rule by being proportional to the finite time, $\Delta\tau = 2T$, that the detector is switched on.

It is a fact that physical detectors can be accelerated linearly and uniformly only for a finite amount of time. Consequently, we can take the switch-on time, $\Delta\tau = 2T$, to be the finite amount of time that the detector is being accelerated.

In the next section (VII.E) we introduce a dynamical wave complex ("acceleron") which also has a finite life time,

$$\Delta\tau = \varepsilon \quad .$$

The existence, identity, and detailed physical properties of this wave complex can be predicted by calculating the interaction between it and a finite-time detector. The interaction between the two evokes a maximum response in the detector if the life times of the two match,

$$\varepsilon \approx 2T \quad .$$

Suppose the detector is in resonance with this wave complex, i.e.

$$E_{fin} - E_{init} \approx \overline{\omega} \quad ,$$

where $\overline{\omega}$ is its characteristic frequency defined in Eq.(105. Then these two systems exchange "boost" energy periodically in a manner analogous to two interacting pendulums. Such a periodic energy exchange would presumably be accessible to experiments. This resonance interaction would yield enough information about the state of this wave complex to allow it being used as a new way of probing the properties of spacetime. This detection process corresponds to using photons to watch planets and comets to obtain information about their positions and velocities for the purpose of probing the properties of spacetime (gravitation). Space limitations forbid us to pursue this line of inquiries in this article.

VII. WAVELETS AND WAVE PACKET HISTORIES

The (U, V)-parametrized family of Minkowski-Bessel distributions constitutes a linear one-to-one transform from the space spanned by orthonormal wavelets to the space of wave packet histories.

A wavelet is a square-integrable function which is localized in phase space, i.e. the function $\phi(\theta)$ and its Fourier transform $\hat{\phi}(\omega)$ are concentrated on small sets. We shall use the term "wavelet" in a sense which is (slightly) more inclusive than that used by the "wavelet theory" community [12]- [14]. Our orthonormal "wavelets" agree with theirs in that "wavelets" are localized in the given domain (say, $-\infty < \theta < \infty$) and the Fourier domain ($-\infty < \omega < \infty$). However, workers in "wavelet theory" restrict the term orthonormal "wavelets" to sequences of functions whose localization in the given domain is described by compression and translation operations applied to a single "mother wavelet" function [15], [16]. As a consequence, this restricts their wavelets to those whose adjacent frequencies in a (wavelet) Fourier series differ from each other by an octave in the Fourier domain. We, on the other hand, include also those which realize the windowed Fourier transform, such as Eqs.(106) and (107) in the ensuing mathematical tutorial.

Either of the wavelets, $\phi(\theta)$ or $\hat{\phi}(\omega)$, determines a unique wave packet history, a solution to the Klein-Gordon equation:

$$\phi^{\pm}(kU, kV) = \int_{-\infty}^{\infty} \hat{\phi}(\omega)^* B^{\pm}_{\omega}(kU, kV)\ d\omega \tag{61}$$

$$= \int_{-\infty}^{\infty} \phi(\theta)^* \frac{1}{\sqrt{2\pi}} e^{\mp ik(Ve^{\theta} + Ue^{-\theta})/2}\ d\theta \quad . \tag{62}$$

As noted in the opening sentence, the correspondence between the set of wave packet histories and the set of square-integrable functions is linear and one-to-one. In fact, the inverse transformation is

$$\hat{\phi}(\omega)^* = \pm \langle B^{\pm}_{\omega}, \phi^{\pm} \rangle \tag{63}$$

$$\phi(\theta)^* = \pm \langle \frac{1}{\sqrt{2\pi}} e^{\mp ik(Ve^{\theta} + Ue^{-\theta})/2}, \phi^{\pm} \rangle \quad . \tag{64}$$

This follows from the Klein-Gordon orthonormality of the Minkowski-Bessel and the plane wave modes:

$$\langle B^{\pm}_{\omega}, B^{\pm}_{\omega'} \rangle \equiv \frac{i}{2} \int_{-\infty}^{\infty} \left[(B^{\pm}_{\omega})^* \frac{\partial}{\partial t} B^{\pm}_{\omega'} - \frac{\partial}{\partial t} (B^{\pm}_{\omega})^* B^{\pm}_{\omega'} \right]\ dz \tag{65}$$

$$= \pm \delta(\omega - \omega') \tag{66}$$

$$\langle B^{+}_{\omega}, B^{-}_{\omega'} \rangle = 0$$

$$\langle \frac{e^{\mp ik(Ve^{\theta} + Ue^{-\theta})/2}}{\sqrt{2\pi}}, \frac{e^{\mp ik(Ve^{\theta'} + Ue^{-\theta'})/2}}{\sqrt{2\pi}} \rangle = \pm \delta(\theta - \theta') \quad .$$

A. The Phase Space

The outstanding virtue of the two transforms, Eqs.(61) and (62) is the Fourier duality of the two sets, $\{\phi\}$ and $\{\hat{\phi}\}$, of square-integrable functions. They serve to represent the Klein-Gordon solutions in two different and mutually exclusive ways: one relative to an inertial frame via plane wave modes, the other relative to the four Rindler quadrants of a pair of accelerated frames via Minkowski-Bessel modes.

This Fourier duality implies the existence of the familiar two-dimensional phase space. As demonstrated in the ensuing tutorial, this space is partitioned by a chosen basis of orthonormal wavelets into equal-area phase space cells, each one of area 2π. This set of wavelets and their Fourier transforms,

$$\{\phi^{\varepsilon}_{j\ell}(\theta)\ :\ \ j, \ell = 0, \pm 1, \pm 2, \cdots\} \tag{67}$$

and

$$\{\hat{\phi}^{\varepsilon}_{j\ell}(\omega)\ :\ \ j, \ell = 0, \pm 1, \pm 2, \cdots\} \tag{68}$$

satisfy the orthonormality condition

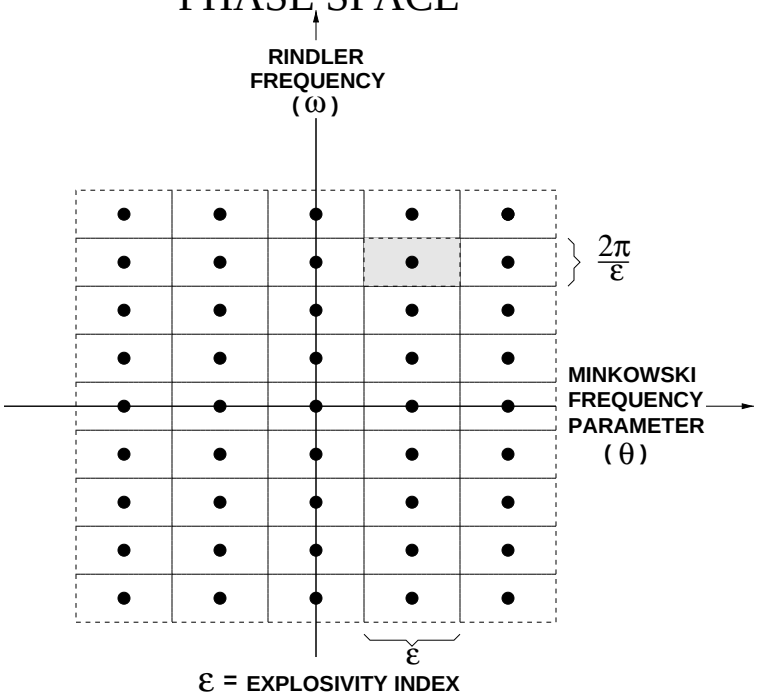

FIG. 8. Two-dimensional phase space spanned by the Minkowski frequency parameter θ (Eq.(7)) and by the Rindler frequency ω. The windowed Fourier basis of orthonormal wavelets (Eqs.(106)-(107)) partitions this space into phase space cells of equal area 2π. The support of each wavelet and its Fourier transform are concentrated horizontally and vertically within each dashed rectangle. A heavy dot locates the amplitude maximum of the corresponding wavelet and its Fourier transform. The shape of the area elements is controlled by the freely adjustable parameter ε. Physically it indicates the rate at which each Klein-Gordon wave packet collapses and explodes.

$$\int_{-\infty}^{\infty} [\phi_{j\ell}^{\varepsilon}(\theta)]^* \phi_{j'\ell'}(\theta)]\ d\theta = \int_{-\infty}^{\infty} [\hat{\phi}_{j\ell}^{\varepsilon}(\omega)]^* \hat{\phi}_{j'\ell'}(\omega)\ d\omega = \delta_{jj'}\delta_{ll'} \quad , \tag{69}$$

and, as pointed out in the ensuing tutorial, they form a complete set. However, its most interesting feature from the viewpoint of physics is the freedom one has in choosing the size of the domain neighborhood on which the wavelet is concentrated. For the wavelet, Eq.(106),

$$\phi_{j\ell}^{\varepsilon}(\theta) \quad \text{this neighborhood is} \quad (\ell - \frac{1}{2})\varepsilon \leq \theta \leq (\ell + \frac{1}{2})\varepsilon, \tag{70}$$

while for its Fourier transform, Eq.(107),

$$\hat{\phi}_{j\ell}^{\varepsilon}(\omega) \quad \text{this neighborhood is} \quad (j - \frac{1}{2})\frac{2\pi}{\varepsilon} \leq \omega \leq (j + \frac{1}{2})\frac{2\pi}{\varepsilon}. \tag{71}$$

The size of these neighborhoods is obviously controlled by the positive parameter $0 < \varepsilon < \infty$.

There are two extreme cases which have physically important consequences:

1. Whenever $\varepsilon \ll 1$, the wavelet basis elements $\phi_{j\ell}^{\varepsilon}(\theta)$ are concentrated in a very small subinterval in the θ-domain. This implies, of course, that their Fourier transforms, $\hat{\phi}_{j\ell}^{\varepsilon}(\omega)$, are very spread out in the ω-domain.

2. Whenever $\varepsilon \gg 1$, the wavelet basis elements $\hat{\phi}_{j\ell}^{\varepsilon}(\omega)$ are concentrated in a very small subinterval in the ω-domain. In that case we know that their inverse Fourier transforms, $\phi_{j\ell}^{\varepsilon}(\theta)$, are correspondingly spread out in the θ-domain. Thus by varying the parameter $0 < \varepsilon < \infty$ one deforms continuously the wavelets $\phi_{j\ell}^{\varepsilon}(\theta)$ from ones which are highly localized in the θ-domain to those whose Fourier transforms, $\hat{\phi}_{j\ell}^{\varepsilon}(\omega)$, are highly localized in the ω-domain. In fact, in the asymptotic limit this localized behavior is proportional to a Dirac delta function.

This process of deformation alters the shape of the phase space cells, whose union makes up the phase space. Assume, as is done in the ensuing tutorial, that this two-dimensional phase space is coordinatized horizontally by

$-\infty < \theta < \infty$ and vertically by $-\infty < \omega < \infty$. Then, as depicted in Figure 9, this deformation corresponds to changing the shape of each phase space area element from being tall and skinny ($\varepsilon \ll 1$) to being short and squatty ($\varepsilon \gg 1$).

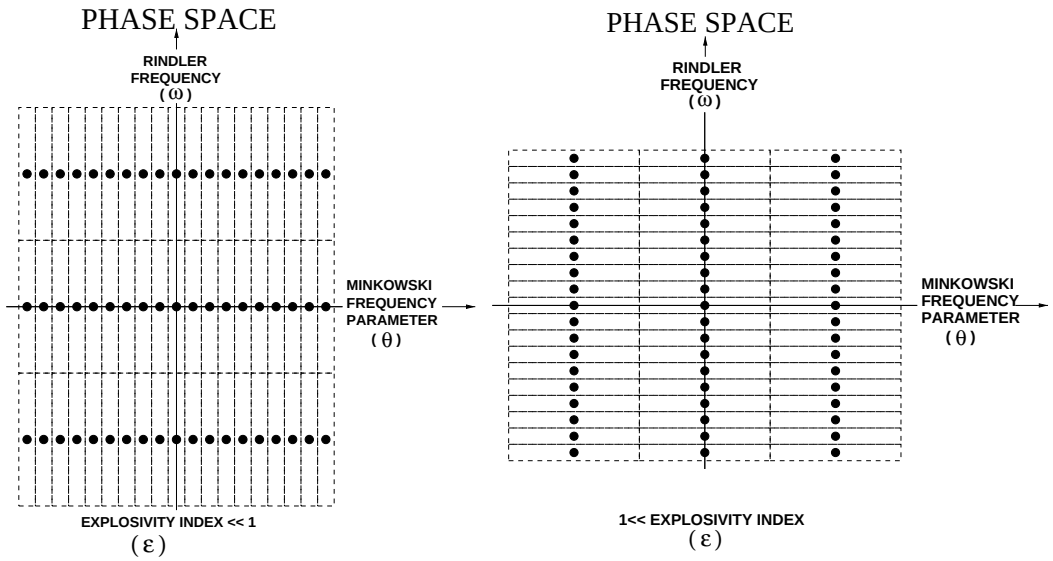

FIG. 9. Two different partitionings of phase space. The elementary phase space areas have the same magnitude, but their shapes are different. They are characterized by the explosivity index ε defined in Figure 8. The tall and skinny elements ($\varepsilon \ll 1$) define Klein-Gordon wave packet histories with well-defined mean Minkowski frequency but indeterminate Rindler frequency. Such wave packets *contract and re-expand non-relativistically* in their respective frames of reference. By contrast, the short and squatty elements ($1 \ll \varepsilon$) define Klein-Gordon wave packet histories with well-defined mean Rindler frequency but indeterminate Minkowski frequency. Such wave packets *collapse and re-explode relativistically* in their respective frames of reference.

B. Complete Set of Smooth Orthonormal Wave Packet Histories

Every complete set of orthonormal wavelets determines a corresponding set of Klein-Gordon orthonormal wave packet histories.

Consider the orthonormal wavelets

$$\phi^{\varepsilon}_{j\ell}(\theta) = \frac{1}{\sqrt{\varepsilon}} \exp\left(-i\frac{2\pi}{\varepsilon} j\theta\right) \times \left\{ \begin{array}{ll} 1 & \text{whenever } (\ell - \frac{1}{2})\varepsilon \le \theta \le (\ell + \frac{1}{2})\varepsilon \\ 0 & \text{whenever } \frac{\varepsilon}{2} < |\ell\varepsilon - \theta| \end{array} \right\} \quad j, \ell = 0, \pm 1, \pm, 2, \cdots \quad , \tag{72}$$

and their Fourier transforms

$$\begin{aligned} \hat{\phi}^{\varepsilon}_{j\ell}(\omega) &= \frac{1}{\sqrt{2\pi\varepsilon}} \int_{(\ell-\frac{1}{2})\epsilon}^{(\ell+\frac{1}{2})\varepsilon} \exp i\left(\omega - \frac{2\pi}{\varepsilon} j\right)\theta \; d\theta \qquad\qquad j, \ell = 0, \pm 1, \cdots \\ &= \frac{1}{\sqrt{2\pi\varepsilon}} \exp i\left(\omega - \frac{2\pi}{\varepsilon} j\right) l\epsilon \times \frac{2\sin\left(\omega - \frac{2\pi}{\epsilon} j\right)\frac{\epsilon}{2}}{\left(\omega - \frac{2\pi}{\epsilon} j\right)}, \end{aligned} \tag{73}$$

These wavelets are taken from the ensuing tutorial, Section VIII.B. The corresponding wave packet histories,

$$\phi^{\varepsilon\pm}_{j\ell}(kU, kV) \equiv \int_{-\infty}^{\infty} \hat{\phi}^{\varepsilon}_{j\ell}(\omega)^* B^{\pm}_{\omega}(kU, kV) \; d\omega \tag{74}$$

$$= \int_{-\infty}^{\infty} \phi^{\varepsilon}_{j\ell}(\theta)^* \frac{1}{\sqrt{2\pi}} e^{\mp ik(Ve^{\theta} + Ue^{-\theta})/2} d\theta \quad j, \ell = 0, \pm 1, \pm 2, \cdots \quad , \tag{75}$$

are Klein-Gordon-orthonormal, and the correspondence itself is obviously one-to-one and linear. Furthermore, the completeness of the set of orthonormal wavelets, i.e.

$$\sum_{j=-\infty}^{\infty}\sum_{\ell=-\infty}^{\infty}\phi^{\varepsilon}_{j\ell}(\theta)\ \phi^{\varepsilon}_{j\ell}(\theta')^{*}=\delta(\theta-\theta') \tag{76}$$

$$\sum_{j=-\infty}^{\infty}\sum_{\ell=-\infty}^{\infty}\hat{\phi}^{\varepsilon}_{j\ell}(\omega)\ \hat{\phi}^{\varepsilon}_{j\ell}(\omega')^{*}=\delta(\omega-\omega') \tag{77}$$

implies the completeness of the corresponding set wave packet histories. This means that *any solution to the Klein-Gordon Eq.(5), say $\psi(kU,kV)$, can be expressed as a linear combination of these histories:*

$$\psi(kU,kV)=\sum_{j=-\infty}^{\infty}\sum_{\ell=-\infty}^{\infty}a_{j\ell}\phi^{\varepsilon+}_{j\ell}(kU,kV)\ +\ b^{*}_{j\ell}\phi^{\varepsilon-}_{j\ell}(kU,kV) \tag{78}$$

where the coefficients are expressed in terms of the Klein-Gordon inner product, Eq.(65),

$$a_{j\ell}=\langle\phi^{\varepsilon+}_{j\ell},\psi\rangle\quad;\quad b^{*}_{j\ell}=-\langle\phi^{\varepsilon-}_{j\ell},\psi\rangle\quad. \tag{79}$$

The most perspicuous feature about the wave packet histories is their dependence on the common parameter $0<\varepsilon<\infty$. When $\varepsilon\ll 1$, and the wavelet $\phi^{\varepsilon}_{j\ell}(\theta)$ is highly localized in the Minkowski frequency (θ) domain, then the wave packet history $\phi^{\varepsilon\pm}_{j\ell}(kU,kV)$ is a long, but finite, wave train travelling with a spacetime velocity whose direction is determined by the localized θ-value of the wavelet. As is well known and is shown in the next subsection, the size of this wave train is not constant. In fact, it contracts, reaches a minimum size, and then re-expands at a rate whose asymptotic value is

$$\frac{v}{c}=\varepsilon\qquad\ll\ 1$$

in the proper rest frame of the wavetrain packet. This process is very gentle, with an appearance very much like that of a diffusive evolution.

When $1\ll\varepsilon$, and the wavelet $\hat{\phi}^{\varepsilon}_{j\ell}(\omega)$ is highly localized in the Rindler frequency (ω) domain, then the wave packet history $\phi^{\varepsilon\pm}_{j\ell}(kU,kV)$ manifests itself in a violent way relative to a globally inertial reference frame. In fact, from the boundary of the history in Figures 5, 6, or 7 one sees that the history consists of a collapse followed by an explosion. This process is characterized by contraction and expansion rates which are relativistic into both the negative and the positive z-direction, and their asymptotic magnitude is

$$\frac{v}{c}=\tanh\frac{\varepsilon}{2\pi}\qquad\approx 1\quad.$$

This asymptotically relativistic expansion (or contraction) makes the process have the appearance of an explosion (or collapse). Indeed, the violence of this evolutionary unfolding is controlled entirely by the positive parameter ε. For this reason it is appropriate to refer to ε as the *explosivity index* of the wave complex, as is done in Figures 8 and 9.

C. Two Asymptotic Limits

A wave packet and a classical particle are similar in that they both refer to a localized property such as mass, or charge, or electromagnetic energy, and so on. This similarity is the means by which one identifies the difference in their degree of localization. Quantitatively one does this with the parameter $0<\varepsilon<\infty$, the "conceptual common denominator", which distinguishes between different kinds of wave packet evolutions. Fundamentally, there are only two of them: the *Inertial Frame Limit*, characterized by $\varepsilon\ll 1$ and the *Rindler Frame Limit* characterized by $1\ll\varepsilon$.

In the "$\varepsilon\ll 1$" limit each wave packet has a (well-defined) group velocity which defines a unique inertial frame. This limit accommodates the familiar concept of a classical particle.

By contrast, in the "$1\ll\varepsilon$" limit there is no such thing as a group velocity, and hence no such thing as an inertial frame defined by parallel world lines [18] of classical particles in a state of free float [17]. Instead, each evolving wave complex is characterized by a Lorentzian Mach-Zehnder interference process whose amplitude splitting, reflection, and interference defines the four Rindler sectors of a pair of oppositely accelerated frames.

1. Inertial Frame Limit

One arrives at the concept of a classical particle by letting $\varepsilon \ll 1$ and then letting the proper rest mass of a quantum become very large. In this limiting process, a wave packet history becomes a particle (or antiparticle) world line with a sharply defined tangent at each sharply defined event. Symbolically we express this circumstance by

$$\lim_{\substack{\varepsilon \ll 1 \\ k \to \infty}} \phi_{j\ell}^{\varepsilon\pm}(kU, kV) = \text{“world line of} \begin{cases} \text{a particle”} & \text{(upper sign)} \\ \text{an antiparticle”} & \text{(lower sign)} \end{cases} \tag{80}$$

The three steps which comprise this process are as follows:
1.) Keeping

$$\frac{2\pi}{\varepsilon} j = \text{fixed and finite}$$

and

$$\ell\varepsilon = \text{fixed} \quad ,$$

evaluate the integral representation, Eq.(75), of the wave packet $\phi_{j\ell}^{\varepsilon\pm}(kU, kV)$ in the asymptotic limit of $\varepsilon \ll 1$. The technique for doing this is straight forward and is described in a tutorial (Section IX: “Wave Packets via Constructive Interference”). Using it, one finds

$$\phi_{j\ell}^{\varepsilon\pm}(kU, kV) = \; A\; e^{iS}, \qquad (\varepsilon \ll 1)$$

where

$$e^{iS} = \exp[\mp ik(Ve^{\overline{\theta}} + Ue^{-\overline{\theta}})/2 + \frac{2\pi}{\varepsilon} j\overline{\theta}] \qquad \overline{\theta} = \ell\varepsilon \tag{81}$$

is a rapidly varying function of spacetime, while the factor A is a gently varying Gaussian envelope of constructive interference whose squared modulus is

$$|A|^2 \propto exp\left\{ -\varepsilon^2 \left(\frac{\partial S}{\partial \overline{\theta}} \right)^2 \left[1 + \left(\varepsilon^2 \frac{\partial^2 S}{\partial \overline{\theta}^2} \right)^2 \right]^{-1} \right\}$$

2.) Use the magnitude of this factor to identify that region of spacetime where the wavepacket amplitude is substantially different from zero. A necessary condition for this to be so is that the squared *constructive interference parameter*

$$\delta^2 \equiv \varepsilon^2 \left(\frac{\partial S}{\partial \overline{\theta}} \right)^2 \left[1 + \left(\varepsilon^2 \frac{\partial^2 S}{\partial \overline{\theta}^2} \right)^2 \right]^{-1} \tag{82}$$

satisfy

$$\delta^2 \leq 1 \quad . \tag{83}$$

The boundary of the spacetime region of constructive interference is characterized by $\delta^2 = 1$. If at an event the wave packet has non-negligible squared modulus, then at that event the inequality, Eq.(83), must prevail. In brief, the locus of events of non-negligible squared modulus is given by

$$\frac{\varepsilon^2}{\delta^2} \left(\frac{\partial S}{\partial \overline{\theta}} \right)^2 - \left(\varepsilon^2 \frac{\partial^2 S}{\partial \overline{\theta}^2} \right)^2 = 1, \qquad \delta^2 \leq 1 \quad . \tag{84}$$

The spacetime region determined by this inequality is the Lorentzian version of what in Euclidean wave optics would be a converging, and then a diverging, Gaussian beam [19]. It is important to note that $\varepsilon \ll 1$ does *not* imply that one may omit the term $\left(\varepsilon^2 \frac{\partial^2 S}{\partial \overline{\theta}^2} \right)^2$. Indeed, $\varepsilon^2 \frac{\partial^2 S}{\partial \overline{\theta}^2}$ becomes non-negligible in the past and in the future. This fact is a

reflection of the fact that the "Lorentzian beam", like its Euclidean analogue, never stays parallel. The perpendicular cross section of the beam increases without limit in the past and in the future.

As already noted, the boundary of this Lorentzian beam is $\delta^2 = 1$. With the help of the plane wave phase in Eq.(81), namely

$$S = \mp k(t - t_0)\cosh\overline{\theta} \mp k(z - z_0)\sinh\overline{\theta} + \frac{2\pi}{\varepsilon}j\overline{\theta} \quad ,$$

this boundary, Eq.(84,) is the pair of conjugate timelike hyperbolas

$$\frac{(\Delta z')^2}{a^2} - \frac{t'^2}{b^2} = 1 \quad , \tag{85}$$

where, first of all

$$a = \frac{1}{k\varepsilon} \tag{86}$$

is the *initial proper width* of the wave packet, secondly

$$\frac{a}{b} = \varepsilon \tag{87}$$

is its *proper (asymptotic) expansion rate*, and finally

$$\Delta z' = (z - z_0)\cosh\overline{\theta} + (t - t_0)\sinh\overline{\theta} \mp \frac{2\pi}{k\varepsilon}j; \qquad \overline{\theta} = \ell\varepsilon \tag{88}$$

is its *proper halfwidth* after an *elapsed proper time*

$$t' = (t - t_0)\cosh\overline{\theta} + (z - z_0)\sinh\overline{\theta} \quad .$$

3.) Taking note of the fact that the squared half width of a wave packet is

$$(\Delta z')^2 = \frac{1}{\varepsilon^2 k^2} + \varepsilon^2 t'^2 \quad , \tag{89}$$

consider the problem of finding *that* wave packet, and its history, for which

$$(\Delta z')^2 = \ minimum \tag{90}$$

relative to $(\Delta z')^2$ of all other wave packets parametrized by $0 < \varepsilon < \infty$.
The history of such a minimal wave packet most closely resembles a particle world line of finite length t'. Such a wave packet has initial size

$$2a = 2\sqrt{\frac{t'}{k}} \quad , \tag{91}$$

expands at the (asymptotic) rate

$$2\frac{a}{b} = 2\sqrt{\frac{1}{t'k}} \ \ (= 2\varepsilon) \tag{92}$$

and after proper time t' has full width

$$2\Delta z'_{min} = 2\sqrt{\frac{2t'}{k}} \quad . \tag{93}$$

Here

$$k = \sqrt{\frac{m^2c^2}{\hbar^2} + k_y^2 + k_x^2}$$

is the Compton wave number of the wave packet of a particle with non-zero transverse motion. With increasing particle mass the expansion rate $\varepsilon = \sqrt{1/t'k}$ tends towards zero, and, with it, the expansion rate and the size of the minimal wave packet. In this limit this corresponds to the razor sharp world line of a classical particle. This circumstance is what is summarized by Eq.(80).

Metaphysically, however, the rest mass of a particle is always finite. Thus the size of its wave packet and the concomitant expansion rate are always non-zero nevertheless. As an example, take the world line of a neutron in a state of rest for the time duration $t'_{conv} = 1$ second in conventional units. The neutron's Compton wave length is $\lambda_n = 2 \times 10^{-14}$ cm. Consequently, its minimum initial wave packet size is

$$2a = 2\sqrt{\lambda_n c t'_{conv}} = 4.6 \times 10^{-2} \ \text{ cm} \ .$$

After one second the full width of this wave packet is

$$2\Delta z_{min} \equiv 2.8a = 6.4 \times 10^{-2} \ \text{ cm} \ ,$$

and it expands at the nonzero rate

$$v_{conv} \equiv 2\frac{a}{b}c = 2\sqrt{\frac{\lambda_n c}{t'_{conv}}} = 5 \times 10^{-2} \ \text{ cm/sec} \ ,$$

which is nonrelativistic.

The establishment, and hence the definition, of an inertial frame is done in terms of Newton's first law of motion. The classically precise definition of an inertial frame is as follows [17]:
A reference frame is said to be an "inertial" or "free-float" or "Lorentz" reference frame in a certain region of space and time when, throughout that region of spacetime – and within some specified accuracy– *every free test particle initially at rest initially at rest with respect to that frame remains at rest, and every test particle initially in motion with respect to that frame continues its motion without change in speed or in direction.*

The fact that every test particle has a finite Compton radius and hence is described by a moving wave packet of non-zero minimal width and expansion rate, implies that an inertial frame cannot be made arbitrarily small. Nevertheless, we adopt the above definition and extend it to quantum mechanics by replacing the (mathematically uncountable) set of test particles with the (countable) complete set of Klein-Gordon-orthonormal wave packet histories

$$\{\phi^{\varepsilon\pm}_{j\ell}(kU, kV) \ : \ j, \ell = 0, \pm 1, \pm 2, \cdots\}, \tag{94}$$

which are governed by the relativistic wave equation (5).

Let us use these wave packet histories to establish an inertial frame. We do this by replacing the parallel particle world lines used by Marzke and Wheeler [18] with corresponding wave packets.

Without specifying the construction of a quantum mechanical clock, we consider for the duration of a finite time interval, say t', an array of N freely floating material particles (resp. anti-particles) which

(i) have the same proper mass

(ii) have no velocity relative to one another

(iii) have a minimal separation which is large enough to allow them to be distinguished by their spatial location.

This separation is the spacing between the contiguous wave packet histories

$$\phi^{\varepsilon\pm}_{1\ell}(kU, kV), \phi^{\varepsilon\pm}_{2\ell}(kU, kV), \cdots, \phi^{\varepsilon\pm}_{N\ell}(kU, kV)$$

for each of these particles (resp. anti-particles). Equation (88) tells us that this separation is

$$\frac{2\pi}{k\varepsilon} = \frac{2\pi}{\varepsilon}\frac{mc}{\hbar} \ .$$

Optimized relative to the time interval t', these wave packets expand at the rate $\varepsilon = \sqrt{1/t'k}$. As a result, their optimal (i.e. minimum) separation is

$$\frac{2\pi}{k\varepsilon} = 2\pi\sqrt{\frac{t'}{k}} \quad (= 2\pi a) \tag{95}$$

The total proper spatial extent of these N freely floating particles is therefore

$$2\pi\sqrt{\frac{t'}{k}}N = 2\pi\sqrt{\frac{t'\hbar}{mc}}N \tag{96}$$

$$\equiv L \quad . \tag{97}$$

They make up a meter rod of length L, whose resolution and accuracy cannot be improved upon except by increasing the mass of its constitutive particles or by decreasing the amount of time that this meter rod is used. More precisely, although the *absolute* accuracy, Eq.(95), used to define an inertial frame is limited by these two quantities, the *relative* accuracy can be increased by making N, and hence the spatial extent L, sufficiently large.

2. Rindler Frame Limit

The behaviour of a nonrelativistically expanding wave packet is interesting. One can make it expand faster by having its minimum proper size, Eq.(86) be smaller (or having its transverse wave number k be smaller). Suppose one keeps increasing ε until the expansion rate, Eq.(87), becomes highly relativistic, i.e. $1 \ll \varepsilon$. Under this circumstance the inertial-frame-limit analysis would no longer apply. Instead, a glance at Eq.(74) tells us that the wave packet $\phi^{\varepsilon\pm}_{j\ell}(kU, kV)$ starts resembling a Minkowski-Bessel mode, and the evolution process of the wave packet starts resembling the Lorentzian Mach-Zehnder interference process, Figure 2, whose details are depicted in Figures 5,6, and 7.

However, this resemblance is a peculiar one: The M-B mode oscillates infinitely rapidly at and near $U = V = 0$, the intersection of the two horizons, while the wave packet $\phi^{\varepsilon\pm}_{j\ell}(kU, kV)$ is smooth at this event, even when $1 \ll \varepsilon$. This persistent discrepancy implies that *each wave packet* bifurcates *into a pair of wave packets, one in Rindler Sector I, the other in Rindler Sector II, which then* re-coalesce *into a single wave packet in F*. This bifurcation-recoalescence process is an interference effect. It is exhibited by each relativistically collapsing and re-exploding wave packet $\phi^{\varepsilon\pm}_{j\ell}(kU, kV)$. Its squared modulus , as calculated in the tutorial of Eq.(122), is controlled by the (squared) *constructive interference parameter*

$$\delta^2 \equiv \Delta^2 \left(\frac{\partial S}{\partial \overline{\omega}}\right)^2 \left[1 + \left(\Delta^2 \frac{\partial^2 S}{\partial \overline{\omega}^2}\right)^2\right]^{-1} \qquad \left(\Delta \equiv \frac{2\pi}{\varepsilon} \ll 1\right) \tag{98}$$

(*Notation:* $\partial/\partial\overline{\omega}$ means first take the partial with respect to ω and then evaluate at it at $\overline{\omega}$.) The region of spacetime where the wave packet has non-negligible amplitude is characterized by the in equality

$$-1 \leq \delta \leq 1 \quad . \tag{99}$$

With the help of Figure 7 one finds that

$$\Delta^2 \frac{\partial^2 S}{\partial \overline{\omega}^2} = \pm \frac{\Delta^2}{\sqrt{\overline{\omega}^2 + k^2 UV}} \tag{100}$$

This term, or rather its square, is negligibly small in Eq.(98) throughout the spacetime region of interest, namely wherever the oscillatory WKB approximation is applicable (away from the hyperbolic boundaries between the classically allowed and the classically forbidden regions in Rindler Sectors I and II). With this approximation, together with Figure 7 and Eqs.(9)-(10) one finds that Eq.(98) is equivalent to one of the straight lines

$$(t - t_0)\sinh\left(\ell\varepsilon + \delta\frac{\varepsilon}{2\pi}\right) + (z - z_0)\cosh\left(\ell\varepsilon + \delta\frac{\varepsilon}{2\pi}\right) = \frac{\overline{\omega}}{k}\frac{V}{|V|}; \qquad \overline{\omega} = \frac{2\pi}{\varepsilon}j \quad j = 0, \pm1, \pm2, \cdots \tag{101}$$

when

$$\begin{aligned} S &\equiv \mathcal{S}^V - \omega\ell\varepsilon \\ &= \omega\ln(\omega + \sqrt{\omega^2 + k^2UV}) - \sqrt{\omega^2 + k^2UV} - \omega\ln k|V| - \frac{\pi}{4} - \omega\ell\varepsilon \quad , \end{aligned}$$

or to

$$(t - t_0)\sinh\left(\ell\varepsilon + \delta\frac{\varepsilon}{2\pi}\right) + (z - z_0)\cosh\left(\ell\varepsilon + \delta\frac{\varepsilon}{2\pi}\right) = -\frac{\overline{\omega}}{k}\frac{U}{|U|} \tag{102}$$

when

$$S \equiv \mathcal{S}^U - \omega\ell\varepsilon$$
$$= \omega \ln(\omega + \sqrt{\omega^2 + k^2UV}) - \sqrt{\omega^2 + k^2UV} - \omega \ln k|U| - \frac{\pi}{4} - \omega\ell\varepsilon \quad .$$

These straight lines form a δ-parametrized family whose parameter is restricted by Eq.(99). As we know, this restriction guarantees that the events on these straight lines lie in those regions of spacetime where the wave packet $\phi^{\varepsilon\pm}_{j\ell}(kU, kV)$ has non-negligible amplitude. As the interference parameter varies from $\delta = -1$ to $\delta = 1$, the family of straight lines "generates" the spacetime domain of constructive interference. Outside this domain the wave packet has exponentially small amplitude.

With the help of Eq.(1) the family of generating lines is represented in Rindler Sector I by

$$\xi \cosh\left(\tau + \ell\varepsilon + \delta\frac{\varepsilon}{2\pi}\right) = \frac{|\overline{\omega}|}{k} \quad , \quad |\delta| \leq 1 \quad .$$

Consequently, the region swept out by this δ-parametrized family consists of the set of events whose intersection with Rindler Sector I equals

$$\{(\xi, \tau) : \ \xi \cosh\left(\tau + \ell\varepsilon + \delta\frac{\varepsilon}{2\pi}\right) = \frac{|\overline{\omega}|}{k}; \ \ |\delta| \leq 1\} \quad .$$

This set is obviously bounded away from the event $U = V = 0$. In fact, its proper distance away from this event is

$$\frac{\overline{\omega}}{k}\frac{1}{\cosh \varepsilon/2\pi} \quad .$$

In Rindler Sector II there exists an inverted image ($U \to -U, \ V \to -V$) of this set. The proper separation between these two sets is therefore

$$\begin{pmatrix} \text{separation between} \\ \text{bifurcated wave} \\ \text{packet histories} \end{pmatrix} = 2\frac{\overline{\omega}}{k}\frac{1}{\cosh \varepsilon/2\pi} \quad . \tag{103}$$

The spacetime between these two sets is an "island of calmness" (zero wave packet amplitude) whose center is the event $U = V = 0$ where every wave packet has strictly zero amplitude.

D. Collapsing Wave Packet Bifurcates: Double Slit

It is qualitatively obvious that a relativistically collapsing wave packet should bifurcate into a pair of distinct wave packets, which upon re-exploding merge into a single relativistically expanding wave complex. The reason is destructive interference between the Minkowski-Bessel modes comprising the wave packet. They lie in a narrow range of Rindler frequencies and, as demonstrated in one of the ensuing tutorials (Section IX), their amplitudes add or cancel depending on the location in spacetime.

Recall that every M-B mode oscillates with infinite rapidity as one approaches the intersection ($U = V = 0$) of the future and past event horizons. This is evident from Figures 5 and 7. When superimposed, such rapidly oscillating amplitudes interfere destructively whenever that superposition extends over a small but finite range of Rindler frequencies. Moreover, that destructive interference becomes perfect as one approaches the event $U = V = 0$ from any direction in spacetime. This event is the center of an island of "total calmness" (zero amplitude) in spacetime. This island, whose spacelike extent is given by Eq.(103), separates the pair of wave packet histories, one in Rindler Sector I, the other in Sector II, before they coalesce into the single history of a relativistically exploding wave packet in Rindler Sector F.The boundary of this packet expands with asymptotic velocity whose magnitude (relative to the center of this packet) is

$$u = \tanh\frac{\varepsilon}{2\pi} \quad ,$$

a fact which follows from Eq.(101) or (102) by letting $\ell = 0$.

On each spacelike slice of elapsed time ($\xi = const.$) in F through this history, this wave complex consists of a pattern of interference. This interference is between the two amplitudes of the bifurcated wave packet amplitudes

from sectors I and II respectively. Thus, in a physically rigorous sense, the two Rindler sectors I and II act as a double slit arrangement which accommodates an interference process between coherent amplitudes passing through two finite spacelike openings separated by the above-mentioned "island of calmness".

Both "double slit" and "Lorentzian Mach-Zehnder interferometer" are accurate terms which describe the spacetime arrangement that gives rise to the interference process $P \to (I, II) \to F$. The difference is that the latter term highlights the reflection process which is brought about in I and II by their respective pseudo gravitational potentials. The former term leaves the nature of this reflection process unspecified.

E. Accelerons

We know that, when $\varepsilon \gg 1$, the wavelet $\hat{\phi}^{\varepsilon}_{j\ell}(\omega)$ is highly localized around a well-defined Rindler frequency, say $\omega = \overline{\omega}$. The concomitant wave packet history is

$$\phi^{\varepsilon\pm}_{j\ell}(kU, kV) = \int_{-\infty}^{\infty} \left[\hat{\phi}^{\varepsilon}_{j\ell}(\omega)\right]^* B^{\pm}_{\omega}(kU, kV)\ d\omega \quad . \tag{104}$$

Consequently, the wave amplitude of $\phi^{\varepsilon\pm}_{j\ell}(kU, kV)$ and that of $B^{\pm}_{\overline{\omega}}(kU, kV)$ are roughly the same functions of spacetime (U, V). A glance at Figures 5,6, or 7 reveals therefore that $\phi^{\varepsilon\pm}_{j\ell}(kU, kV)$ is non-zero in F, in P, as well as in those regions of Rindler sectors I and II which lie between the two conjugate hyperbolas ("boundaries of evanescence") and the event horizons.

These mathematical properties of this wave amplitude express the following physical meaning:
First of all, relative to any globally inertial reference frame $\phi^{\varepsilon\pm}_{j\ell}(kU, kV)$ expresses the history of a wave complex which is *finite*. The two timelike hyperbolic boundaries of evanescence, indicated in Figures 5,6, and 7 guarantee this. Second, this wave complex collapses *relativistically to a minimum size*, the proper distance between the two hyperbolic boundaries, before it *explodes relativistically*. Third, relative to accelerated observers in Rindler Sectors I and/or II, the wave complex is an approximately *static* entity. Its Rindler lifetime is very long:

$$\Delta\tau \approx \varepsilon \gg 1$$

During this time interval the boundary, and hence the size

$$\xi = \frac{2\overline{\omega}}{k}; \qquad \overline{\omega} = \frac{2\pi}{\varepsilon} j \quad j = 0, \pm 1, \pm 2, \cdots \tag{105}$$

of this entity is approximately static. In this article the boundary consists of two parallel planes parallel to the y and x coordinates; in other words, we have a static slab [20] whose proper thickness is Eq.(105). In its *interior* the wave field oscillates with mean Rindler frequency $\overline{\omega}$.

Thus $\phi^{\varepsilon\pm}_{j\ell}(kU, kV)$ is a field configuration which

- vibrates
- is localized along the z-direction, and
- has a static boundary

What is the field amplitude (or the quantum states) of this oscillating entity? This is a question one would ask relative to the two accelerated frames, Rindler I and II, and it pertains to the field amplitudes and phases of these two sectors. The answer is mathematically simple [6], but it needs to be justified also physically, i.e. related to observations accessible to an inertial observer. *If one can do this*, then the above oscillating entity has a fourth property, namely $\phi^{\varepsilon\pm}_{j\ell}(kU, kV)$

- is a Klein-Gordon degree of freedom with quantum states of excitation.

We shall call a wave complex with the above four properties an *acceleron*. This is because of the accelerative nature of its boundary relative to an inertial frame.

In summary, there are two kinds of wave mechanical building blocks in nature. Wave packets ($\varepsilon \ll 1$) and accelerons ($\varepsilon \gg 1$). Wave packets express the particle-like properties of ponderable matter. (The deflection of light by the sun is an example.) This is because these properties are measured by an observing apparatus based on the intrinsic attributes of a free float frame. By contrast, accelerons express those "complementary" properties of ponderable

matter (Amplification of light passing through on accelerated dielectric, see Section X.B), which are measured by an observing apparatus based on the attributes of a pair of frames accelerating uniformly and linearly into opposite directions.

The wave packet properties and the acceleron properties are "complementary" in the sense of wave mechanics. Indeed, wave packets have phase space area representatives which are tall and skinny ($\varepsilon \ll 1$), while accelerons have phase space representatives which are short and squatty ($\varepsilon \gg 1$), as in Figure 9. The vertical and the horizontal phase space coordinates quantify properties (Minkowski Frequency and Rindler Frequency) which are experimentally mutually exclusive. Their dichotomic nature is captured by the phrase "complementary".

VIII. MATHEMATICAL TUTORIAL: PHASE SPACE OF SQUARE-INTEGRABLE FUNCTIONS

A. Why

The motivation for introducing the phase space of square-integrable functions is both physical and mathematical.

The mathematical motivation comes from the necessity that we comprehend the square-integrable test functions and their Fourier transforms from a *single* point of view. This means that the classification of these functions be based on their behavior on the given domain concurrent with the behaviour of their transform on the Fourier domain.

The physical motivation comes from the necessity that we identify the Klein-Gordon dynamics in terms of orthonormal degrees of freedom which are localized both in their spacetime-translation-induced properties (momentum) and in their Lorentz-boost-induced properties (boost "energy"). The momentum and the boost "energy" domains are Fourier complementary attributes. One indicates an inertial frame, the other a pair of frames accelerating into opposite directions. Consequently, these complementary attributes seem to constitute a metaphysically insurmountable either-or duality. Nevertheless, comprehending nature demands that we represent any given Klein-Gordon solution in terms of orthonormalized degrees of freedom which capture *both* attributes in the manner dictated by the Fourier transform.

The phase space of functions square-integrable on the real line not only fulfills this demand but also answers the following two questions:

1. How does one construct Klein-Gordon orthonormal wave histories?

2. How does one obtain a physical classification of the solutions to the relativistic wave equation?

The "physical" classification is to include not only the circumstance of low dispersion wave packets tracing out a narrow and straight world tube, but also the circumstance of wave packets with such high dispersion that they explode relativistically and thus have a non-trivial internal dynamics.

B. Phase Space Construction

Instead of developing that phase space in its most general mathematical form, we shall illustrate its basic nature with an archetypical construction. This is a three step process:

(1) First, exhibit a complete set of orthonormal wave packet functions and their Fourier transforms.

This first step is facilitated by noting that there is a practical and general method for constructing square-integrable functions which are orthonormal on the real line $-\infty < \theta < \infty$. To use this method, one needs to pick only a single square-integrable function with an easily specifiable property stipulated by the following theorem:

For any square-integrable function $\phi(\theta)$ the set $\{\phi_\ell(\theta) \equiv \phi(\theta - \frac{2\pi}{\varepsilon}\ell) : \quad \ell = 0, \pm 1, \pm 2, \cdots\}$ is an orthonormal system, i.e.

$$(\phi_\ell, \phi_{\ell'}) \equiv \int_{-\infty}^{\infty} \phi_\ell(\theta)^* \phi_{\ell'}(\theta)\ d\theta = \delta_{\ell\ell'} \quad ,$$

if and only if the Fourier transform of $\phi(\theta)$,

$$\hat{\phi}(\omega) = \frac{1}{\sqrt{2\pi}} \int_{-\infty}^{\infty} \phi(\theta) e^{i\omega\theta} \quad d\theta$$

satisfies

$$\sum_{n=-\infty}^{\infty} |\hat{\phi}(\omega + \frac{2\pi}{\varepsilon} n)|^2 = \frac{\varepsilon}{2\pi} \quad .$$

This powerful theorem, well known to workers in wavelet theory [13], captures the key idea behind the success in using windowed Fourier transforms (among others) to construct orthonormal wavelets. Indeed, let us apply this theorem to the windowed function

$$\phi(\theta) = \frac{1}{\sqrt{\varepsilon}} \exp\left(-i\frac{2\pi}{\varepsilon} j\theta\right) \times \begin{cases} 1 & -\frac{\varepsilon}{2} \le \theta \le \frac{\varepsilon}{2} \\ 0 & 0 < \frac{\varepsilon}{2} < |\theta| \end{cases}$$

Here j is an arbitrary integer.
The Fourier transform of this function is

$$\hat{\phi}(\omega) = \frac{1}{\sqrt{2\pi\epsilon}} \frac{2\sin\left(\omega - \frac{2\pi}{\epsilon} j\right) \frac{\epsilon}{2}}{\left(\omega - \frac{2\pi}{\epsilon} j\right)}$$

and the sum mentioned in the theorem is

$$\begin{aligned} \sum_{n=-\infty}^{\infty} |\hat{\phi}(\omega + \frac{2\pi}{\varepsilon} n)|^2 &= \frac{1}{2\pi\epsilon} \sum_{n=-\infty}^{\infty} \frac{4\sin^2\left(\omega - \frac{2\pi}{\epsilon} j + \frac{2\pi}{\epsilon} n\right) \frac{\epsilon}{2}}{\left(\omega - \frac{2\pi}{\epsilon} j + \frac{2\pi}{\epsilon} n\right)^2} \\ &= \frac{\varepsilon}{2\pi} \sin^2 \frac{\omega\varepsilon}{2} \sum_{n=-\infty}^{\infty} \frac{1}{\left(\frac{\omega\varepsilon}{2} + \pi n\right)^2} \\ &= \frac{\varepsilon}{2\pi} \quad \text{for all} \quad -\infty < \omega < \infty. \end{aligned}$$

This means we can use the theorem. It guarantees us that the system of exponentials windowed along the θ-axis,

$$\phi_{j\ell}(\theta) = \frac{1}{\sqrt{\varepsilon}} \exp\left(-i\frac{2\pi}{\varepsilon} j\theta\right) \times \left\{ \begin{array}{ll} 1 & \text{whenever } (\ell - \frac{1}{2})\varepsilon \le \theta \le (\ell + \frac{1}{2})\varepsilon \\ 0 & \text{whenever } \frac{\varepsilon}{2} < |\ell\varepsilon - \theta| \end{array} \right\} \quad j, \ell = 0, \pm 1, \pm, 2, \cdots \quad , \tag{106}$$

and their Fourier transforms

$$\begin{aligned} \hat{\phi}_{j\ell}(\omega) &= \frac{1}{\sqrt{2\pi\varepsilon}} \int_{(l-\frac{1}{2})\epsilon}^{(l+\frac{1}{2})\varepsilon} \exp i\left(\omega - \frac{2\pi}{\varepsilon} j\right) \theta \; d\theta \qquad\qquad j, \ell = 0, \pm 1, \cdots \\ &= \frac{1}{\sqrt{2\pi\varepsilon}} \exp i\left(\omega - \frac{2\pi}{\varepsilon} j\right) l\epsilon \times \frac{2\sin\left(\omega - \frac{2\pi}{\epsilon} j\right) \frac{\epsilon}{2}}{\left(\omega - \frac{2\pi}{\epsilon} j\right)}, \end{aligned} \tag{107}$$

form an ε-parametrized family of sets of wave packets orthonormal on the Fourier-complementary domains $-\infty < \theta < \infty$ and $-\infty < \omega < \infty$:

$$\int_{-\infty}^{\infty} \phi_{j\ell}(\theta)^* \phi_{j'\ell'}(\theta) \; d\theta = \int_{-\infty}^{\infty} \hat{\phi}_{j\ell}(\omega)^* \hat{\phi}_{j'\ell'}(\omega) \; d\omega = \delta_{jj'}\delta_{ll'} \quad . \tag{108}$$

(2) Second, assemble the function domain and the corresponding Fourier domain into a two-dimensional phase plane, and use the localized nature of these functions to partition this plane into a set of mutually exclusive and jointly exhaustive phase space cells.

This step consists of taking note of the localized nature of the orthonormal basis functions and their Fourier transforms. From their definitions one finds that

$$\phi_{j\ell}(\theta) \text{ is concentrated in } (\ell - \frac{1}{2})\varepsilon < \theta < (\ell + \frac{1}{2})\varepsilon,$$

while its Fourier transform

$$\hat{\phi}_{j\ell}(\omega) \text{ is concentrated in } (j - \frac{1}{2})\frac{2\pi}{\varepsilon} < \omega < (j + \frac{1}{2})\frac{2\pi}{\varepsilon}.$$

It follows that the phase space of square-integrable functions

(i) consists of the two-dimensional plane spanned by the cartesian coordinates $-\infty < \theta < \infty$ and $-\infty < \omega < \infty$ and

(ii) is partitioned into elements of area

$$\varepsilon \times \frac{2\pi}{\varepsilon} = 2\pi$$

whose horizontal width ε and vertical height $\frac{2\pi}{\varepsilon}$ are the separations between the adjacent wave packets $\phi_{j\ell}(\theta)$ and $\hat{\phi}_{j\ell}(\omega)$. The centers of these area elements constitute the lattice work of points

$$\{\ (\theta,\omega) = \left(\ell\varepsilon, j\frac{2\pi}{\varepsilon}\right) : \quad \ell, j = 0, \pm 1, \pm, 2, \cdots\ \}$$

where the modulus of the wavelets $\phi_{j\ell}(\theta)$ and $\hat{\phi}_{j\ell}(\omega)$ have their respective maximum values.

Roughly speaking, the o.n. wavelets $\phi_{j\ell}(\theta)$ and their Fourier transforms $\hat{\phi}_{j\ell}(\omega)$ cause the phase space to be covered completely with a set of rectangular tiles of equal area whose shape is determined by the parameter $0 < \varepsilon < \infty$. This is depicted in Figure 8

(3) Third, use the completeness and the orthonormality properties to assign to these cells the respective Fourier coefficients of any given square-integrable function.

This final step consists of taking note of the completeness of each set of o.n. wavelets. Thus any square-integrable function $f(\theta)$ and its Fourier transform $\hat{f}(\omega)$ is a linear combination of these wavelets

$$f(\theta) = \sum_{j=-\infty}^{\infty} \sum_{\ell=-\infty}^{\infty} \phi_{j\ell}(\theta) \int_{-\infty}^{\infty} \phi^*_{j\ell}(\theta') f(\theta') \ \ d\theta' \tag{109}$$

$$\hat{f}(\omega) = \sum_{j=-\infty}^{\infty} \sum_{\ell=-\infty}^{\infty} \hat{\phi}_{j\ell}(\omega) \int_{-\infty}^{\infty} \hat{\phi}^*_{j\ell}(\omega') \hat{f}(\omega') \ \ d\omega' \tag{110}$$

It is remarkable and obvious (because they are Fourier transforms of each other) that even though these two functions are superficially different, their Fourier coefficients are the *same*:

$$\int_{-\infty}^{\infty} \phi^*_{j\ell}(\theta') f(\theta') \ \ d\theta' = \int_{-\infty}^{\infty} \hat{\phi}^*_{j\ell}(\omega') \hat{f}(\omega') \ \ d\omega' \tag{111}$$

$$\equiv c_{j\ell} \tag{112}$$

Consequently, the Fourier transform pair has the form

$$f(\theta) = \sum_{j=-\infty}^{\infty} \sum_{\ell=-\infty}^{\infty} c_{j\ell} \phi_{j\ell}(\theta) \tag{113}$$

and

$$\hat{f}(\omega) = \sum_{j=-\infty}^{\infty} \sum_{\ell=-\infty}^{\infty} c_{j\ell} \hat{\phi}_{j\ell}(\omega)\ . \tag{114}$$

These two representations imply that any square-integrable function, together with its Fourier transform, is represented geometrically by assigning each common Fourier coefficient $c_{j\ell}$ to its phase space area element located at $(\theta,\omega) = (\ell\varepsilon, j\frac{2\pi}{\varepsilon})$. Even though the magnitude of the area of all these elements is the same, namely 2π, their shape depends on the parameter ε. As shown in Figure 9, when $\varepsilon \ll 1$, they are compressed along the horizontal and stretched along the vertical, and vice versa when $1 \ll \varepsilon$.

C. Exploding Wave Packets: Relativistic Internal Dynamics ($\varepsilon \gg 1$)

When $1 \ll \varepsilon$ then each phase space elements gets mapped by Eq.(74) into a relativistically collapsing and re-exploding wave complex whose spacetime support is indicative of the partitioning of spacetime into the four Rindler sectors, Figure 1. The collapse and the re-explosion is so violent as to preclude a wave mechanical description of a classical particle relative to an inertial frame. Instead, the physical (i.e. measurable) properties of the evolution process must be described in terms of the Lorentz version of the Mach-Zehnder interference process of Section *I*. For every pair of integers (j, ℓ) the Klein-Gordon solution $\phi^{\varepsilon\pm}_{j\ell}(kU, kV)$ expresses such a process.

The wave complex $\phi^{\varepsilon\pm}_{j\ell}(kU, kV)$ is the relativistic antithesis of any one of the familiar plane wave packets. Each complex

1. has an indeterminate direction in the $z-t$ plane but has a well-defined mean Rindler ("boost") frequency

$$\overline{\omega} = \frac{2\pi}{\varepsilon} j \quad , \quad j = 0, \pm 1, \pm 2, \cdots \quad ,$$

2. has a Rindler time life span of order

$$\Delta\tau \approx \varepsilon \gg 1 \quad ,$$

which is centered around

$$\tau = \ell\varepsilon \quad , \quad \ell = 0, \pm 1, \cdots \quad ,$$

3. has an ill-defined group velocity which is less sharp the larger ε is, and

4. has a very large asymptotic velocity spread whose magnitude in the wave packet rest frame is

$$\Delta u = 2 \tanh \frac{\varepsilon}{2\pi} \quad \text{("relativistic velocity spread")} \quad . \tag{115}$$

IX. MATHEMATICAL TUTORIAL: WAVE PACKETS VIA CONSTRUCTIVE INTERFERENCE

Let us describe and apply a general method which facilitates the extraction of the physical properties of wave packets histories from their integral representations, Eqs.(74) and (75). Their explicit form is

$$\phi^{\varepsilon\pm}_{j\ell}(kU, kV) \equiv \int_{-\infty}^{\infty} \left[\frac{1}{\sqrt{2\pi\varepsilon}} \exp i \left(\omega - \frac{2\pi}{\varepsilon} j \right) l\epsilon \times \frac{2 \sin \left(\omega - \frac{2\pi}{\epsilon} j \right) \frac{\epsilon}{2}}{\left(\omega - \frac{2\pi}{\epsilon} j \right)} \right]^* B^{\pm}_{\omega}(kU, kV) \; d\omega \tag{116}$$

$$= \int_{(\ell - \frac{1}{2})\varepsilon}^{(\ell + \frac{1}{2})\varepsilon} \left[\frac{1}{\sqrt{\varepsilon}} \exp \left(-i \frac{2\pi}{\varepsilon} j\theta \right) \right]^* \frac{1}{\sqrt{2\pi}} e^{\mp ik(Ve^{\theta} + Ue^{-\theta})/2} d\theta \quad j, \ell = 0, \pm 1, \pm 2, \cdots \quad , \tag{117}$$

These are different representations of one and the same wave packet $\phi^{\varepsilon\pm}_{j\ell}(kU, kV)$. Note that each representation has its own window function. In Eq.(116) there is the "sinc" function whose half width in the ω-domain is $2\pi/\varepsilon$. By contrast in Eq.(117) there is the "square wave pulse" function whose width in the θ-domain is ε. Consequently, for large ε the representation (116) has a narrow window and the representation (117) a wide window, while for small ε it is the other way around.

A. Overview

The method guarantees success for both large-ε (relativistically collapsing and exploding) and for small-ε (slowly contracting and expanding) wave packets. The basic philosophy underlying this method is akin to the method of steepest descent, and it is the same for Eq.(116) and for Eq.(117) In both cases the given integral is replaced to an excellent approximation by a Gaussian integral. The method employed here is a three step procedure.

1. Replace the phase modulated window functions (in Eq.(116) or in Eq.(117), whichever one has the narrower maximum) with its equivalent phase modulated Gaussian window function.

2. With the location of the maximum as the reference point, expand the phase of the modes in a Taylor series. The narrowness of the Gaussian window function guarantees that terms which are cubic or higher may be omitted without affecting the accuracy of the integral.

3. The outcome of steps 1 and 2 is a Gaussian integral. Evaluate it and thereby obtain a slowly varying amplitude times a rapidly varying phase factor. This product is the sought-after history of a wave complex.

From this modulated Gaussian extract the key properties of the wave packet history:

1. The amplitude locates those events in spacetime where wave field quanta can be found.

2. By contrast, the rapidly varying phase factor controls the interference with other wave packets.

B. Evaluation of the Integral

We shall forego applying this method to the plane waves because the properties of the resulting slowly expanding ($\varepsilon \ll 1$) wave packets are generally known. Instead, let us apply it to the relativistically exploding ($1 \ll \varepsilon$) wave packets, Eq.(116).

We replace its Rindler frequency sinc envelope in Eq.(116),

$$\frac{\sin\left(\frac{2\pi}{\epsilon}j-\omega\right)\frac{\epsilon}{2}}{\left(\frac{2\pi}{\epsilon}j-\omega\right)} \ ,$$

with the equivalent Gaussian window

$$\frac{\pi}{\Delta}\exp\left\{-\frac{(\frac{2\pi}{\varepsilon}j-\omega)^2}{2\Delta^2}\right\} \equiv f(\omega) \quad . \tag{118}$$

Here

$$\Delta \equiv \frac{2\pi}{\varepsilon} \ll 1$$

is the effective half width of this window. It has the same maximum amplitude and the same width at its inflection points as the sinc function. The corresponding phase modulated Gaussian window function,

$$\hat{\phi}_{j\ell}(\omega) \approx \frac{1}{\sqrt{2\pi\varepsilon}} e^{i\left(\frac{2\pi}{\varepsilon}j-\omega\right)\ell\varepsilon} f(\omega) \quad ,$$

takes the place of the exact window function in the history of the wave complex, Eq.(116). Its integral representation is

$$\begin{aligned}\phi^{\varepsilon\pm}_{j\ell}(kU,kV) &= \int_{-\infty}^{\infty}\left[\frac{1}{\sqrt{2\pi\varepsilon}} e^{i\left(\frac{2\pi}{\varepsilon}j-\omega\right)\ell\varepsilon} f(\omega)\right] \ \mathcal{A}(\omega)e^{iS_\omega} \quad d\omega \\ &\equiv \frac{1}{\sqrt{2\pi\varepsilon}}\int_{-\infty}^{\infty}\mathcal{A}(\omega)f(\omega)e^{iS} \ d\omega \end{aligned} \tag{119}$$

where

$$S \equiv \mathcal{S}_\omega - \omega\ell\varepsilon \tag{120}$$

is the *total* phase and the function $\mathcal{S}_\omega$ is one of the four possible signed WKB phases, given in Figure 7. The phase factor e^{iS} is a rapidly varying function of ω. The slowly varying function $\mathcal{A}(\omega)$ is the WKB-approximate M-B mode amplitude (also given in Figure 7), which is nearly constant across the narrow Gaussian ω-window defined by $f(\omega)$, Eq.(118)

Note that the analytic expressions in Figure 7 apply only to the "classically allowed" region of spacetime, i.e. where $k^2UV < \omega^2$ between the two conjugate time-like hyperbolas, the boundaries of the regions of evanescence. We have

not given, and we need *not* concern ourselves with those regions of spacetime where the wave packets have evanescent behaviour. This is because in those regions the wave packets have exponentially small amplitudes.

The maximum of the Gaussian window, Eq.(118) is located at the Rindler frequency

$$\overline{\omega} = \frac{2\pi}{\varepsilon} j \qquad j = 0, \pm 1, \pm 2, \cdots \quad .$$

The truncated Taylor series of the WKB phase around this point is

$$S(\omega) = S(\overline{\omega}) + \frac{\partial S}{\partial \overline{\omega}}(\omega - \overline{\omega}) + \frac{1}{2}\frac{\partial^2 S}{\partial \overline{\omega}^2}(\omega - \overline{\omega})^2 \quad .$$

Introduce this phase into the to-be-evaluated integral, Eq(119) This integral now has the form

$$\int_{-\infty}^{\infty} \exp(\alpha z^2 + \beta z)\, dz = \sqrt{\frac{\pi}{-\alpha}} \exp(-\frac{\beta^2}{4\alpha}) \qquad (Re\ \alpha < 0) \quad .$$

Use this result and find that the expression for the wave packet is

$$\phi_{j\ell}^{\varepsilon\pm}(kU, kV) = \left((2\pi^3)^{1/2} \sqrt{\frac{1+i\sigma}{1+\sigma^2}} \exp\left[-\frac{\Delta^2}{2} \left(\frac{\partial S}{\partial \overline{\omega}} \right)^2 \left(\frac{1+i\sigma}{1+\sigma^2} \right) \right] \right) \times \left(\frac{1}{\sqrt{2\pi\varepsilon}} \mathcal{A}(\overline{\omega}) e^{iS(\overline{\omega})} \right) \quad . \tag{121}$$

Here

$$\begin{aligned} \sigma &\equiv \frac{\partial^2 S}{\partial \overline{\omega}^2} \Delta^2 \\ &= \pm \frac{\Delta^2}{\sqrt{\overline{\omega}^2 + k^2 UV}} \end{aligned}$$

is negligibly small throughout those regions of spacetime where the WKB approximation is applicable, i.e. away from the (hyperbolic) boundaries between the classically allowed and the classically forbidden regions in Rindler sectors I and II.

The utility of this explicit expression for the wave packet history is the mathematical transparency of its squared modulus,

$$|\phi_{j\ell}^{\varepsilon\pm}(kU, kV)|^2 = const. \frac{\mathcal{A}^2(\overline{\omega})}{\sqrt{1+\sigma^2}} \exp\left\{ -\Delta^2 \left(\frac{\partial S}{\partial \overline{\omega}} \right)^2 \left[1 + \left(\Delta^2 \frac{\partial^2 S}{\partial \overline{\omega}^2} \right)^2 \right]^{-1} \right\} \quad . \tag{122}$$

It answers the mathematical question: In what regions of spacetime does the wave packet history have non-negligible intensity? If $\phi_{j\ell}^{\varepsilon\pm}(kU, kV)$ refers to the wave function of a single particle (resp. antiparticle), then the squared modulus answers the physical question: Where in spacetime is there a non-zero probability for finding a particle (resp. antiparticle)? The exponent of Eq.(122) gives the necessary condition. The probability is non-zero in those regions of spacetime where the squared *constructive interference parameter*

$$\delta^2 \equiv \Delta^2 \left(\frac{\partial S}{\partial \overline{\omega}} \right)^2 \left[1 + \left(\Delta^2 \frac{\partial^2 S}{\partial \overline{\omega}^2} \right)^2 \right]^{-1} \qquad \left(\Delta \equiv \frac{2\pi}{\varepsilon} \ll 1 \right) \tag{123}$$

satisfies

$$\delta^2 \leq 1 \quad .$$

This condition is violated in those regions of spacetime where $\phi_{j\ell}^{\varepsilon\pm}(kU, kV)$ has negligible amplitude.

X. DOUBLE SLIT INTERFERENCE

From a future historical perspective the last quarter of the Twentieth century will undoubtedly be marked by the intrigue generated by the acceleration temperature. What other formulas in physics, besides the acceleration-induced thermal energy

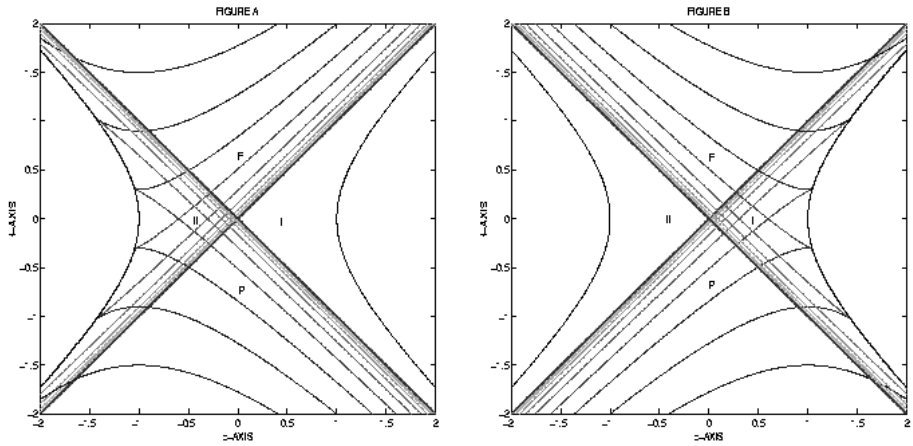

FIG. 10. Double slit interference of two waves modes entering and emerging from a pair of accelerated frames. In reality the two figures should be superimposed, one on top of the other, in order to show the composite phase fronts of a single relativistically collapsing and exploding wave packet. However, for clarity, we show the two interfering waves separately, one passing through Rindler Sector I (FIGURE B), the other through Rindler Sector II (FIGURE A). The interference occurs in Rindler Sector F, where the two waves meet and superpose to form a resultant wave.
The process of each partial wave passing through its respective spacetime sector (I and II) is a reflection process. Each figure depicts the WKB phase fronts being reflected by the pseudo-gravitational potential. Note that the direction of propagation of the wave mode is perpendicular (in the Lorentz sense) to its phase fronts. FIGURE B pictures the reflection process $P \to I \to F$, which is expressed by the wave $\mathcal{A}\exp[i\mathcal{S}^V] + \mathcal{A}\exp[-i\mathcal{S}^U]$, the WKB expression for B^+_ω in Figure 7a. The incident wave $\mathcal{A}\exp[-i\mathcal{S}^U]$, which propagates from P towards the boundary ($UV = \omega^2$) of evanescence in Im represented in the figure by the isograms of $\mathcal{S}^U$. Similarly, the reflected wave $\mathcal{A}\exp[i\mathcal{S}^V]$, which propagates from the boundary of evanescence in I to the future F, is represented by the isograms of the phase $\mathcal{S}^V$. Note that the incident and the reflected phase contours intersect the boundary in a perpendicular way.
In an analogous way, FIGURE A pictures the reflection process $P \to II \to F$, which is expressed by the wave $e^{-\pi\omega}\mathcal{A}\exp[-i\mathcal{S}^U] + e^{-\pi\omega}\mathcal{A}\exp[i\mathcal{S}^V]$, the WKB expression for B^+_ω in Figure 7a. The superposed process $P \to (I, II) \to F$ manifests itself as interference in Rindler Sector F, where the phase fronts in FIGURE A overlap with those in FIGURE B.

$$kT = \frac{\hbar}{c}\frac{g}{2\pi} \quad ,$$

can rival $E = \hbar\omega$ and $E = c^2 m$ in its ubiquity, in its fundamental role as indicated by the two most important constants of nature, $\hbar$ and c, and in its implication for gravitation via the surface gravity

$$g = \frac{c^3}{4MG}$$

of black holes?

No wonder the interaction between uniformly accelerated quantum system and the quantized wave field has been the object of such intense investigations. The ostensive goal has been to identify the wider framework which would accommodate our understanding of the acceleration temperature as given by the Davies-Unruh formula. As a reward, this framework would identify the iceberg which presumably lies hidden under the acceleration temperature.

A. Accelerated "Detectors"

To achieve this goal, the exclusive strategy has been to have the accelerated quantum system consist of a kind of localized thermometer which interacts with the thermal ambience in Rindler sector I (or II).

This strategy has been used for the purpose of determining how an accelerated point particle with internal quantum states responds to a relativistic field, and, conversely, how the field responds to the internal dynamics of such a "detector".

The simplicity of first order quantum perturbation theory has pretty much established agreement about the response of an accelerated "detector" to the thermal ambience of the Minkowski vacuum. However, predictions about

measurable effects of the "detector" dynamics on the field are not characterized by such simplicity. In fact, analyses are characterized by higher order perturbation theory [21,22] and/or fairly specialized tools whose sophistication [23–26] is not commensurate with the simplicity of the phenomenon.

However, an astonishingly simple and fruitful formulation is possible in terms of interfering wave amplitudes. Suppose one recognizes that the distinguishing feature of a Minkowski-Bessel mode propagating from the past P to the future F is (i) that it splits itself into a pair of disjoint amplitudes which subsequently recombine coherently in F, and (ii) that this recombination is an interference between the two amplitudes from the two Rindler Sectors I and II. This (Lorentzian) double slit interference process implies that any quantum system situated in one or both of these slits (i.e. Rindler sectors) has a measurable effect on the interference.

B. Amplification by an Accelerated Dielectric

Instead of considering the familiar single accelerated point particle with its internal quantum states, take the case of a set of accelerated oscillators in, say, Rindler sector I. Let each oscillator be a charge bound harmonically to an ion of an accelerated dielectric medium. Each oscillator amplitude produces an electric polarization in the dielectric medium. The manner in which these oscillators respond collectively to an electromagnetic field is characterized by the electric susceptibility and hence by the refractive index of the accelerated medium. The Maxwell field equations, with its displacement field related to its electric field by this refractive index, give an exact long wave description of the interaction between the coherent motion of the oscillators and the electromagnetic field.

Next consider a monochromatic (i.e. of Rindler frequency ω) electromagnetic wave entering Rindler sector I from the past event horizon ($V = 0, U < 0$), as shown in Figures 6, 7, or 10 for example. In the process of being reflected by the pseudo-gravitational potential, this wave ($\propto \mathcal{A}\exp[-i\mathcal{S}^U] \sim e^{-i(\omega\tau - ln\xi)}$) first goes through the accelerated dielectric one way, and then, after reflection, this wave comes back ($\propto \mathcal{A}\exp[i\mathcal{S}^V] \sim e^{-i(\omega\tau + ln\xi)}$) the other way. In so doing the wave acquires a well-defined phase shift. Its magnitude, $2\delta_I(\omega)$ (not to be confused with the interference parameters δ of Eqs.(82) and (98)), depends on the thickness of the dielectric as well as on the Rindler frequency of the wave. The phase shifted wave escapes from Rindler sector I through its event horizon. Upon entering Rindler sector F, the wave combines with a wave which suffered an analogous phase shift, $\delta_{II}(\omega)$, in Rindler sector II. Thus the particle amplitude, which in P is

$$B^+_\omega = e^{-\pi\omega}\mathcal{A}e^{i\mathcal{S}^V} + \mathcal{A}e^{-i\mathcal{S}^U} \quad ,$$

becomes a phase-altered amplitude which in F is equal to

$$e^{-\pi\omega}\mathcal{A}e^{i\mathcal{S}^U}e^{i2\delta_{II}} + \mathcal{A}e^{-i\mathcal{S}^V}e^{i2\delta_I} \tag{124}$$

$$= \left\{ i\frac{\sin(\delta_{II} - \delta_I)}{\sinh\pi\omega} e^{i(\delta_{II}+\delta_I)} \right\} B^-_\omega + \left\{ \frac{e^{\pi\omega}e^{i2\delta_I} - e^{-\pi\omega}e^{i2\delta_{II}}}{\sinh\pi\omega} \right\} B^+_\omega \tag{125}$$

The coefficient of the mode B^-_ω has become nonzero. This shows that the antiparticle amplitude expressed by the first term

$$\Delta\mathcal{A}(\omega) = i\frac{\sin(\delta_{II} - \delta_I)}{\sinh\pi\omega} e^{i(\delta_{II}+\delta_I)} \tag{126}$$

depends on the relative phase $\delta_{II}(\omega) - \delta_I(\omega)$. The antiparticle amplitude oscillates as a function of this relative phase difference. This oscillatory behavior is the interference between the two partial waves emerging from I and II.

The antiparticle amplitude, and hence the amplified mode (creation of quanta), observed in F is therefore due to the difference in the refractive indices of the dielectric media in I and II.

XI. CONCLUSION

The best way of summarizing this article is by starting to compare the motion of a particle as governed by classical mechanics via

$$\frac{d^2x^\mu}{ds^2} + \Gamma^\mu_{\alpha\beta}\frac{dx^\alpha}{ds}\frac{dx^\alpha}{ds} = 0 \quad , \tag{127}$$

or equivalently [27], [28] by

$$\frac{\partial S}{\partial x^\alpha}\frac{\partial S}{\partial x^\beta}g^{\alpha\beta} \; + \; m^2 = 0 \quad \text{plus} \quad \left(\begin{array}{c} \text{“the principle of} \\ \text{constructive interference”} \end{array} \right) \; ,$$

with the motion of a particle as governed by wave mechanics via

$$\frac{\partial^2\psi}{\partial t^2} - \frac{\partial^2\psi}{\partial z^2} + (k_x^2 + k_y^2 + m^2)\psi = 0.$$

One recalls that the classical mechanical description of the free-float (“inertial”) motion of spinless particles is the high mass limit obtained from a very special set of wave packet solutions to the Klein-Gordon equation. Each wave packet must contract and expand at an asymptotically non-relativistic rate, i.e. its explosivity index ε must be much smaller than one (Sections VII.B and VII.C.1). In that case each wave packet is characterized by its proper Minkowski frequency, which in quantum mechanics is the particle's Compton frequency. Increasing this frequency results in (a) the reduction of the particle's wave packet to the location of the wave packet crest obtained from the principle of constructive interference, (b) the reduction of the world tube of the wave packet to the razor-sharp history of a classical particle, and thus (c) the assignment of a needle-sharp tangent vector to each point event on this razor-sharp world line.

The identification of the explosivity index (ε) of a complete set of Klein-Gordon wave packet histories permits us to grasp a new aspect of relativistic wave mechanics:
Consider relativistically expanding wave packets which are characterized by a common explosivity index which is very large. Each of their evolutions is an interference process which takes place in the nature-given Lorentzian Mach-Zehnder interferometer of the four Rindler sectors P, I, II, and F. This process, nature's spacetime version of the double slit interference process, lends itself to a simple mathematical description (Section VII), and is summarized by

$$P \rightarrow (I, II) \rightarrow F \quad ,$$

i.e. amplitude splitting in P (Figure 5), reflections in I and II (Figures 6 and 10), and amplitude recombination, i.e. interference, in F (Figures 7 and 10).

Roughly speaking, this process is the Fourier dual (Section VII) of the familiar process of a low-ε wave packet contracting and re-expanding slowly as it traces out its history in an inertial frame of reference. In the limit of large mass, one recovers the classical mechanics, Eq.(127), of a free particle from the *low-*ε and hence inertial-frame-observed wave packet history. What is the nature and the utility of the large mass limit of the *high-*ε and hence Rindler-frame-observed wave packet histories? Space limitations demand that we consign the answer to this question to a separate paper.

Our path through the wave mechanical landscape leading to nature's spacetime interferometer has been paved with the *Minkowski-Bessel modes* and the *Klein-Gordon orthonormal wave packets* constructed from them. The key markers along this path have been the *phase space* induced by these wave packets and the *Lorentz version of the Mach-Zehnder interferometer* induced by the Minkowski-Bessel modes. Travelling along this path, we got a better understanding of the physical role of finite-time detectors, and caught a glimpse of amplification of radiation scattered by an inhomogeneous accelerated dielectric.

XII. ACKNOWLEDGEMENT

The author appreciates the pleasant discussions, which were both stimulating and valuable, with Vladimir Belinski, Nikolai Narozhny, and L. Sriramkumar during the 8th Marcel Grossmann Meeting in Jerusalem. The author also would like to thank Derek Gerlach for several valuable remarks and making available his MATLAB expertise.

---

[1] See, e.g., M. Born and E. Wolf, *Principles of Optics*, sixth edition, (Pergamon Press, Elmsford, N.Y., 1980), p.312

[2] See, e.g., J.A. Wheeler in *MATHEMATICAL FOUNDATIONS OF QUANTUM THEORY* edited by A.R. Marlow (Academic Press, Inc., New York, 1978)p9-48; see also J.A. Wheeler, Figure 4, in *Quantum Theory and Measurement* edited by J.A. Wheeler and W.H. Zurek (Princeton University Press, Princeton, N.J., 1983), p.182-213

[3] P. Candelas and D. Deutsch, Proc.E Roy.Soc.**A 354**,79 (1977)

[4] F.J. Alexander and U.H. Gerlach, gr-qc/99100086 ; Phys. Rev. **D 44**,3887 (1991) exhibit the TE and TM wave equations in terms of gauge-invariant potentials.

[5] A.Higuchi, G.E.A. Matsas, and D. Sudarsky, Phys. Rev. **D 46**, 3450 (1992)
[6] U.H. Gerlach, gr-qc/9910107 at http://xxx.lanl.gov ; "Acceleration-induced carrier of the imprints of gravitation" in *Proc. of the Eighth Marcel Grossmann Meeting on General Relativity*, Jerusalem, June 23-27, 1997, edited by Tsvi Piran (World Scientific, Singapore, 1999), 806-808; "Quantum mechanical carrier of the imprints of gravitation", Phys.Rev. **D 57**, 4718-4723 (1998)
[7] See, e.g., N.D. Birrel and P.C.W. Davies, *Quantum fields in curved space* (Cambridge University Press, Cambridge, 1982) p115-116
[8] I.M. Gelfand and G.E. Shilov,*Generalized Functions*, Volume 1, translated from Russian by Eugene Saletan (Academic Press, Inc., New York, 1964)
[9] Section 5.11 in C.W. Misner, K.S. Thorne, and J.a. Wheeler, *GRAVITATION* (W.H. Freeman and Co., San Francisco, 1973)
[10] Chapter 1 in R.P. Feynman and A.R. Hibbs, *Quantum Mechanics and Path Integrals*, (McGraw-Hill Book Company, New York, 1965)
[11] A.Higuchi, G.E.A. Matsas, and C.B. Peres, Phys. Rev. **D 48**, 3731 (1993)
[12] Special Issue on "Wavelets", edited by I. Daubechies and J. Kovacevic, Proc. IEEE **84**, pp505-688 (1996)
[13] A.K. Louis, P. Maass, A. Rieder, *Wavelets: Theorie und Anwendungen*, (B.G. Teubner, Stuttgart) (1994)
[14] I. Daubechies, *Ten Lectures on Wavelets*, (Society for Industrial and Applied Mathematics, Philadelphia) (1992)
[15] A. Cohen and J. Kovacevic, Proc. IEEE **84**, 514 (1996)
[16] N. Hess-Nielsen and M.V. Wickerhauser Proc. IEEE **84**, 514 (1996)
[17] E.F. Taylor and J. A. Wheeler, *SPACETIME PHYSICS*; Second Edition (W.H. Freeman and Co., New York, 1992) Chapter 2
[18] R.F. Marzke and J.A. Wheeler in *GRAVITATION AND RELATIVITY* edited by H.-Y. Chiu and W.F. Hoffmann (W.A. Benjamin, Inc., New York, 1964) Chapter 4
[19] See, for example, Figure 6.5 in A. Yariv, *Quantum Electronics, 2nd Edition* (John Wiley and Sons, Inc., New York 1975)
[20] The extension to spherical wave packets, which are localized in all three dimensions, depends on the introduction of *spherical* Rindler coordinates. They are introduced in gr-qc/9910106 at http://xxx.lanl.gov or in "Paired Accelerated Frames" in *Proc. of the Seventh Marcel Grossmann Meeting on General Relativity*, Stanford, USA, July 24-30, 1994, edited by Robert T. Jantzen and G. Mac Keiser (World Scientific, Singapore, 1996); U.H. Gerlach, Int. Jour. Mod. Phys.**A 11**, 3667 (1996); This last reference contains three errata: (i) On page 3668, line 6, the word "existent" should be substituted for the word "existence". Without this substitution the parenthetical definition becomes meaningless. (ii) The whole paragraph in the middle of page 3670 is a misplaced version of the Caption to Figure 1. Consequently, this paragraph should be deleted. (iii) The corrected sentence at the very end of Section 7 (on page 3686) should read "... the spinor transformation which relates Eq.(5.15) to Eq.(5.18)." The above account of these three errata will save the curious reader the task of tracking them down in: ibid., Int. Jour. Mod. Phys.**A 11**, 643 (1997); a correct reprint of this article is also posted at http://math.ohio-state.edu/∼gerlach
[21] W.G. Unruh and R.M. Wald, Phys.Rev. D **29**,1047 (1984)
[22] S. Massar and R. Parentani, Phys. Rev. **D 54**, 7426 (1996)
[23] P.G. Grove, Class. Quantum Grav. **3** 801 (1986)
[24] D. Raine, D. Sciama, P.G. Grove, Proc. Roy. Soc. Lond. A **435**, 205 (1991)
[25] W.G. Unruh, Phys.Rev. D **29**,1047 (1992)
[26] F. Hinterleitner, Ann. Phys. (N.Y.) **226**, 165 (1993)
[27] The Appendix of E.A. Power and Wheeler, Rev. Mod. Phys. **29**, 480 (1957) reprinted in J.A. Wheeler, *TOPICS IN MODERN PHYSICS, VOL. I: Geometrodynamics*, (Academic Press, New York, 1962)
[28] U.H. Gerlach, Phys. Rev. **177**, 1929 (1969)